MOX-Report No. 79/2023

A diffuse interface model of tumour evolution under a finite elastic confinement

Agosti, A.; Bardin, R.; Ciarletta, P.; Grasselli, M.

MOX, Dipartimento di Matematica
Politecnico di Milano, Via Bonardi 9 - 20133 Milano (Italy)

mox-dmat@polimi.it https://mox.polimi.it

A diffuse interface model of tumour evolution under a finite elastic confinement

Abramo Agosti, Riccardo Bardin, Pasquale Ciarletta and Maurizio Grasselli

Abstract. Diffuse interface models have gained a growing interest in cancer research for their ability to investigate the mechano-biological features during tumour progression and to provide simulation tools for personalised anti-cancer strategies at an affordable computational cost. Here we propose a diffuse interface model for tumour evolution which accounts for an interfacial structure mimicking a finite elastic confinement at the tumour boundary, possibly due either to a localised elastic stress induced by host tissue displacements, or collagen remodelling in the peritumoral area. This model consists of a partial differential equation of the Cahn–Hilliard type, with degenerate mobility, single-well potential, and an elastic nonlocal term acting as the effect of a membrane confinement in the chemical potential. Using mixture theory, we derive the corresponding governing equations from thermodynamic principles based on realistic physical and biological assumptions. First, we introduce a suitable regularized problem in order to deal with the degeneracy set of the mobility and the singularity of the potential. For this problem we find a weak solution and provide a regularity result. Then we establish suitable *a priori* estimates which are uniform with respect to the regularization parameters. Passing to the limit in the regularized problem, we prove existence results for different classes of weak solutions to the original problem. Finally, we propose a continuous Galerkin Finite-Element discretization of the problem, where the positivity of the discrete solution is enforced through a variational inequality. Numerical simulations in a two-dimensional domain are also discussed in three test cases for illustrative purposes.

1. Introduction

Cancer is a multi-factorial disease displaying not only with a wide genotypic and phenotypic variability but also a marked ability to sense and to respond to chemo-mechanical cues during all its progression stages [54]. In the last few decades, mathematical modelling has emerged as a useful tool to aid medical researchers shedding light on the key mechano-biological features underlying solid tumour dynamics [25,60]. In particular, diffuse interface approaches have attracted a growing interest for their ability to provide multi-physic models that are robust, thermodynamically consistent and allow to deliver

2020 Mathematics Subject Classification. Primary 35Q92, 65N30; Secondary 92C17.
Keywords. Diffuse interface model, tumor growth, Cahn-Hilliard equation, nonlocal elasticity, degenerate mobility, single well potential, continuous Galerkin approximation..

in-silico numerical simulations at an affordable computational cost [53]. Such models are based on the so-called Cahn–Hilliard equation, which was first proposed in 1958 by J.W. Cahn and J.E. Hilliard [15, 17] as a phenomenological model for phase separation in binary solutions due to an interplay between the entropy mixing and demixing effects due to aggregation, also observed in cell biology [28, 41]) and in several other contexts (see, e.g., [12, 29]).

Here, we propose a novel solid tumour model in which the cancerous mass behaves as a saturated mixture of a cancerous phase, made by cellular aggregates behaving as an elastic fluid, and a healthy phase consisting of healthy cells, extracellular matrix (ECM) and water. We assume that the interface separating the two phases is diffuse: each volumetric element of tissue picked up in the separating layer hosts a volumetric fraction of both the solid and the liquid phase, simultaneously. The mass balance equation for each component of the mixture can be written as a continuity equation with a flux $\mathbf{J}$, namely

$$\frac{\partial \varphi}{\partial t} + \nabla \cdot \mathbf{J} = 0 \tag{1.1a}$$

$$\mathbf{J} = -b(\varphi)\nabla F'(\varphi), \tag{1.1b}$$

where $\varphi = \varphi(\mathbf{x}, t) \in [0, 1]$ represents the concentration (volume fraction) of one component in the binary solution. Typically, the spatial variable $\mathbf{x}$ takes value in a bounded domain Ω with a sufficiently smooth boundary, while t ranges in a given bounded time interval $0 < t < T < \infty$. In equation (1.1b), $b(\varphi)$ is a mobility coefficient that can be constant but in general is a tensor-valued function of φ. Moreover, $F(\varphi)$ is the Landau grand potential defined for instance by

$$F(\varphi) = E \int_\Omega \left[\frac{\gamma^2}{2} |\nabla \varphi|^2 + \psi(\varphi) \right] d\mathbf{x}, \tag{1.2}$$

where E is the elastic modulus of the cancerous phase (units Pa), γ^2 is a positive material parameter related to the interface thickness separating the two phases (units m^2), and $\psi(\varphi)$ is a homogeneous free energy density (per unit volume), representing the intermixing and adhesion forces between the tumour and the host tissue. Following [1, 14] we will adopt a single-well Lennard-Jones type potential of the form

$$\psi(\varphi) = -(1 - \varphi^*) \ln(1 - \varphi) - \frac{\varphi^3}{3} - (1 - \varphi^*) \frac{\varphi^2}{2} - (1 - \varphi^*)\varphi. \tag{1.3}$$

We refer to Section 2.1, for a complete description of this potential. In particular, see Remark 2.1 for the definition of φ^*. The main novelty of the present work is accounting for the presence of an interfacial elastic confinement, mimicking the presence of an elastic membrane encapsulating the tumour boundary. The presence of such a finite elastic effect have been observed experimentally both *ex-vivo* and *in-vivo*, either due to stress generation induced by host tissue displaced during growth or due to collagen remodelling in the ECM at the tumour periphery [65].

For this purpose, we complement the expression of the Landau grand potential (1.2) with a quadratic term accounting for such an elastic contribution. Under suitable physical hypotheses that will be discussed in the following section, the Landau grand potential takes the form

$$F(\varphi) = E\int_\Omega \left(\psi(\varphi) + \frac{\gamma^2}{2}|\nabla\varphi|^2\right) d\mathbf{x} + \frac{k}{\gamma^2}\left(\int_\Omega |\nabla\bar{\varphi}|^2 d\mathbf{x}\right)^{-2}\left[\int_\Omega [H_\lambda(\varphi) - H_\lambda(\bar{\varphi})]\, d\mathbf{x}\right]^2, \tag{1.4}$$

where k (units N/m) is the elastic constant of the cell membranes, and H_λ is a Heaviside-type function. The additional term accounts for the displacement of the host tissue with respect to a threshold value $\lambda \in (0,1)$. Indeed, $H_\lambda(\varphi) - H_\lambda(\bar{\varphi})$ is the signed characteristic function of the domain subset involved in the displacement, taking value 1 where the cellular tissue is expanded with respect to the initial configuration $\bar{\varphi}$, and value -1 where it is contracted. The term $\gamma\int_\Omega|\nabla\bar{\varphi}|^2\, d\mathbf{x}$ is the surface area of the cell distribution in the reference configuration. Hence, the quantity

$$\frac{1}{\gamma}\left(\int_\Omega |\nabla\bar{\varphi}|^2\, d\mathbf{x}\right)^{-1}\int_\Omega [H_\lambda(\varphi) - H_\lambda(\bar{\varphi})]\, d\mathbf{x}$$

represents the total normal displacement around the interface.

1.1. Contribution beyond the state-of-the-art

Aside from the original application to binary alloys introduced in [3, 5], diffuse interface approaches have been extended, among the others, to ternary mixtures in [58], multi-component polymeric systems in [55], mixtures with different heat conductivities in [57], and phase separation in solder alloys in [26]: Later applications concern lithium-ion batteries [66], modelling nano-porosity during de-alloying [32], inpainting of binary images [9, 10], and even the formation of Saturn's rings in [64].

Due to its Eulerian standpoint, the mixture approach is particularly suited to deal with binary flows [39, 52], and multi-phase fluid flows, where a multiphasic Cahn–Hilliard equation is coupled with a Navier-Stokes system [11, 44–46]. Moreover, regarding fluid flows, recent studies considered computational methods for the Cahn–Hilliard equation applied to a Taylor flow in micro/macro-channels [33] and to two-layer flow in channels with sharp topographical features, as in [67]. However, the diffuse interface approach has been remarkably extended to include solid phases behaving as deformable elastic continua [38], and to describe pattern formation in biological and ecological systems, as in [43, 51]. Notable contributions are [35], where the Cahn–Hilliard equation is coupled to the system of linear elasticity, and [2, 34], where it is coupled with viscoelastic systems with large deformations for describing phase separation in presence of elastic interactions between their constituents. An alternative approach along this direction is the *diffuse*

domain approach, introduced in [20, 21] to describe the dynamics of the elastic membrane in tumour growth models avoiding the need to introduce the vector displacement and deformation tensor variables in the system dynamics. In this latter approach, linear elasticity effects are described by the evolution of auxiliary scalar phase field variables associated to the indicator function of the membrane that satisfy the Cahn–Hilliard equation. We point out that the approach introduced in [20, 21] provides an elastic energy that is not translation invariant and a coupled system of local Cahn–Hilliard equations. In particular, a term of the form $\int_\Omega \left(I_M(\mathbf{x},t) - I_M(\mathbf{x},t_0)\right)^2 \, d\mathbf{x}$, where $I_M(\mathbf{x},t)$ is the auxiliary variable associated to the indicator function of the membrane, is introduced in the free energy of the system. Given a translation of the membrane from time t_0 to time t, the latter term is not equal to zero, as depicted in Figure 1. Our framework follows the main ideas of the diffuse domain approach to describe linear elasticity through the evolution of proper phase field variables: in particular, the function $H_\lambda(\varphi)$ in (1.4) is associated to the auxiliary variable $I_M(\mathbf{x},t)$ in the diffuse domain approach. Since $H_\lambda(\varphi)$ depends on the phase field variable φ itself, we don't need to introduce auxiliary variables to the system dynamics to describe elastic effects in the mixture. Moreover, the energy contribution associated to the elastic displacement in (1.4) is invariant under translations, as depicted in Figure 1. Indeed, for an overall translation (with mass conservation) of the tumor configuration, the term $H_\lambda(\varphi) - H_\lambda(\bar{\varphi})$ gives a null contribution when integrated over Ω. We also note that

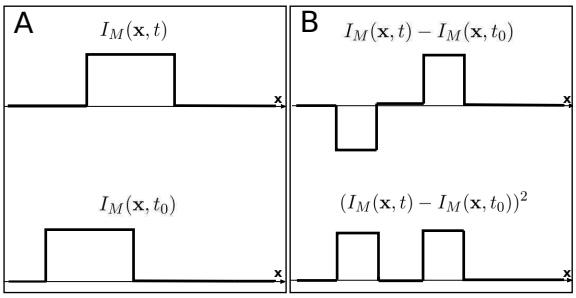

Figure 1. Representation of a translation with mass conservation for the tumor configuration. Panel **A** (left column): indicator function $I_M(\mathbf{x},t_0)$ of the tumor at time t_0 (bottom) and its translation $I_M(\mathbf{x},t)$ at time t (top). Panel **B** (right column): difference of the indicator functions at time t_0 and t (top), and difference of the same functions squared (bottom).

in our approach, differently from the diffuse domain approach, the free energy (1.4) leads to a non-local Cahn–Hilliard equation.

From a purely mathematical point of view, it is worth citing some pioneering contributions that have provided seminal results that we will adapt for the mathematical analysis of our model. Theoretical aspects of equation (1.1), in the case where the mobility is a positive constant and ψ is a smooth double-well potential, have been investigated in [31], while for the logarithmic potential we refer to [22]. If the mobility vanishes at the pure phases and ψ is of logarithmic type, existence of a weak solution (in a suitable sense), to

a boundary value problem including the Cahn–Hilliard equation, has been established in [30], with the interpretation of the sharp interface limit given in [16]. For further details and other contributions, the interested reader is referred to the comprehensive review [56].

1.2. Outline

This article is structured as follows. The model is derived in section 2 illustrating and justifying the related assumptions and simplifications, after introducing the proper functional and the numerical frameworks. Section 3 is devoted to the existence and regularity of a weak solution to a suitably defined initial value boundary value problem for the derived nonlocal equation of the Cahn-Hilliard type. In section 4 we propose a continuous Galerkin Finite–Element discretization of the above problem and we discuss the results of numerical simulations of three different test case to illustrate the effect of the elastic confinement on tumour progression and pattern formation.

2. Preliminaries

In this section we describe the model derivation, providing the biological and physical assumptions which allow to derive a nonlocal variant of (1.1) through the application of mixture theory. Moreover, we present the functional and the numerical frameworks of our analysis.

2.1. Model derivation and assumptions on the mobility and on the potential

We first discuss a multi-phase diffuse-interface mechanical framework which will be the constitutive background of the tumour growth model. The main idea is that tumour cell aggregates can be modelled as ensembles of deformable balloons in contact with each other, the extracellular space being filled by the organic liquid and by the ECM, as in [14].

The general structure of the mixture theory underlying our model can be found for instance in [4, 40]. We consider a binary, saturated, closed, and incompressible mixture, composed by a tumour phase φ_c of proliferating cancerous cells and a healthy phase φ_l of host cells, water and ECM. The saturation constraint reads $\varphi_c + \varphi_l = 1$. In the following, the equations will be written in terms of the tumour phase $\varphi = \varphi_c$, and thus $\varphi_l = 1 - \varphi$. Moreover, the mixture is closed, meaning that the mass transfer rates between the phases are matched. In the end, the incompressibility constraint can be written requiring the average velocity field to to be divergence-free

$$\nabla \cdot (\varphi_c \mathbf{v}_c + \varphi_l \mathbf{v}_l) = \nabla \cdot [\varphi \mathbf{v}_c + (1 - \varphi)\mathbf{v}_l] = 0. \tag{2.1}$$

The resulting governing differential equation is a continuity equation that needs to be closed providing a constitutive law for the phase velocities. The derivation can be carried out following [19], but with modified parameters in accordance with the following assumptions:

(1) Mass flux due to chemotactic movements is neglected and the cells motility is assumed to be isotropic.

(2) The main source of energy dissipation in the system is the viscous drag interaction due to relative motion between the two phases. Such a friction parameter is indicated with D and it is measured in $\mathrm{Pa} \cdot \mathrm{s} \cdot \mathrm{m}^{-2}$.

(3) The diffusion-reaction equation for the nutrient uptake is not incorporated.

(4) The mixture velocity $\mathbf{v}$, that is the average phase velocity weighted by the corresponding volumetric fractions, is considered equal to $\mathbf{0}$, since we investigate the very viscous regime, where the centre of mass of the mixture does not move.

(5) The Landau grand potential functional F includes a nonlocal term modelling the elastic contribution due to tissue movements (see [62] for details on thermodynamic potentials).

For thermodynamic compatibility, we use Onsager's variational principle [27] to enforce the principle of maximum dissipation rate of the free energy. Thus, we compute the stationary points of the Rayleighian functional $\mathcal{R}$, defined as :

$$\mathcal{R} = W + \frac{dF}{dt},$$

with respect to the phase velocities, where W is the energy dissipation and F is the Landau grand potential of the system. Thanks to assumption (2), the energy dissipation functional is given by

$$W = \frac{1}{2}\int_\Omega D\varphi(\mathbf{v}_c - \mathbf{v}_l)\cdot(\mathbf{v}_c - \mathbf{v}_l)d\mathbf{x}, \tag{2.2}$$

meaning that the dissipation is originated only by the relative velocity of the phases, and the friction coefficient D represents a Stokes viscosity coefficient per unit surface. Moreover, from hypothesis (4) we write the Landau grand potential functional as in (1.4). By standard manipulations, we end up with a Darcy's law for the velocity of the cellular phase [13]:

$$\mathbf{v}_c = -\frac{(1-\varphi)^2}{D}\nabla\mu, \tag{2.3}$$

where

$$\mu = F'(\varphi) = \psi'(\varphi) - \gamma^2\Delta\varphi + \frac{2k}{\gamma^2}\left(\int_\Omega |\nabla\bar{\varphi}|^2 d\mathbf{x}\right)^{-2} H'_\lambda(\varphi)\int_\Omega [H_\lambda(\varphi) - H_\lambda(\bar{\varphi})]\, d\mathbf{x}. \tag{2.4}$$

The resulting continuity equation for our model reads

$$\begin{cases} \dfrac{\partial\varphi}{\partial t} - \nabla\cdot[b(\varphi)\nabla\mu] = 0 \\ \mu = \psi'(\varphi) - \gamma^2\Delta\varphi + \dfrac{2k}{\gamma^2}\left(\displaystyle\int_\Omega |\nabla\bar{\varphi}|^2 d\mathbf{x}\right)^{-2} H'_\lambda(\varphi)\int_\Omega [H_\lambda(\varphi) - H_\lambda(\bar{\varphi})]d\mathbf{x}, \end{cases}$$

where

$$b(\varphi) = \frac{\varphi(1-\varphi)^2}{D} \tag{2.5}$$

is the degenerate cell mobility. This expression of the mobility is consistent with the choice (2.2) of the energy dissipation functional W and the derivation of the law for the phase velocity (2.3). For physical consistency and because of cell adhesion mediated by inter-cellular proteins, cell-cell interactions should be attractive at a moderate cell volume fraction and repulsive at higher densities. Hence, there exists a threshold value φ^* corresponding to a homeostatic state, as the volumetric fraction at which the local intercellular forces vanish. This condition is modelled by assuming

$$\psi'(\varphi^*) = 0.$$

For $\varphi < \varphi^*$, cells are attracted to each other and $\psi'(\varphi) \leq 0$, while for $\varphi > \varphi^*$ forces are repulsive and $\psi'(\varphi) > 0$. Above this threshold, repulsive forces tends to infinity as $\varphi \to 1$, when the cancerous cells fill the entire volume (see [14] for further details). In order to account for this physical and biological constraints, we use a phenomenological form of $\psi'(\varphi)$ based on biological observation as in [4, 14, 18, 19]:

$$\psi'(\varphi) = E\frac{\varphi^2(\varphi-\varphi^*)}{1-\varphi} \qquad \varphi > 0. \tag{2.6}$$

More precisely, setting $E = 1$ without loss of generality, we take a Lennard-Jones type potential (see [19, 23, 47])

$$\psi(\varphi) = \psi_1(\varphi) + \psi_2(\varphi), \tag{2.7}$$

where

$$\psi_1(\varphi) = -(1-\varphi^*)\ln(1-\varphi) \tag{2.8}$$

$$\psi_2(\varphi) = -\frac{\varphi^3}{3} - (1-\varphi^*)\frac{\varphi^2}{2} - (1-\varphi^*)\varphi. \tag{2.9}$$

Remark 2.1. Let E be the Young modulus of the cancerous phase, then:

$$E = -E_{\min}\frac{1-\tilde{\varphi}}{\tilde{\varphi}^2(\varphi^*-\tilde{\varphi})},$$

where $(\tilde{\varphi}, E_{\min})$ are the coordinates of the minimum of $\psi'(\varphi)$, with φ^* and $\tilde{\varphi}$ connected by the following relation [14]:

$$\frac{(1-\tilde{\varphi})(3\tilde{\varphi}-2\varphi^*)}{\tilde{\varphi}(\varphi^*-\tilde{\varphi})} = 1.$$

In summary, the resulting model consists of a fourth-order nonlocal Cahn–Hilliard type equation of the form

$$\begin{cases} \dfrac{\partial \varphi}{\partial t} + \nabla \cdot \mathbf{J} = 0 \\ \mathbf{J} = -b(\varphi)\nabla \mu \\ \mu = \dfrac{\delta F}{\delta \varphi} = \psi'(\varphi) - \gamma^2 \Delta \varphi + \dfrac{2k}{\gamma^2} \left(\displaystyle\int_\Omega |\nabla \bar{\varphi}|^2 d\mathbf{x} \right)^{-2} H'_\lambda(\varphi) \int_\Omega [H_\lambda(\varphi) - H_\lambda(\bar{\varphi})] d\mathbf{x}, \end{cases} \tag{2.10}$$

where

- $\varphi \in [0,1]$ is the volume fraction of cancerous cells in the mixture;
- $b(\varphi)$ is the cellular mobility, given by (2.5);
- $\psi(\varphi)$ is the single-well potential chosen to model cell-cell attractive and repulsive forces;
- the elastic nonlocal effects are incorporated into the Landau grand potential functional (1.4) as a global contribution driven by the boundary displacements of the tumour cells. For H_λ we choose the following C^∞-regularization of the step function:

$$H_\lambda(\varphi) = \begin{cases} 0 & \varphi \le 0 \\ \dfrac{2\tanh^2 \varphi}{\tanh^2 \lambda} - \dfrac{\tanh^4 \varphi}{\tanh^4 \lambda} & 0 < \varphi \le \lambda \\ 1 & \varphi > \lambda. \end{cases} \tag{2.11}$$

Consider now (2.10), and set

$$\kappa = \frac{2k}{\gamma^2} \left(\int_\Omega |\nabla \bar{\varphi}|^2 d\mathbf{x} \right)^{-2} \tag{2.12}$$

$$A^\lambda(\varphi) = \int_\Omega [H_\lambda(\varphi) - H_\lambda(\bar{\varphi})] \, d\mathbf{x} \tag{2.13}$$

for the sake of simplicity, and endow it with initial and no-flux boundary conditions. Thus, the total mass is conserved. The resulting initial and boundary value problem is

$$\begin{cases} \dfrac{\partial \varphi}{\partial t} = \nabla \cdot [b(\varphi)\nabla \mu] & \text{in } \Omega_T := \Omega \times (0,T) \\ \mu = \psi'(\varphi) - \gamma^2 \Delta \varphi + \kappa A^\lambda(\varphi) H'_\lambda(\varphi) & \text{in } \Omega_T \\ \varphi(\mathbf{x}, 0) = \varphi_0(\mathbf{x}) & \text{in } \Omega \\ \nabla \varphi \cdot \boldsymbol{\nu} = b(\varphi)\nabla \mu \cdot \boldsymbol{\nu} = 0 & \text{on } \partial\Omega \times (0,T), \end{cases} \tag{2.14}$$

where $\Omega \subset \mathbb{R}^d$, $d = 1, 2, 3$ is a given bounded domain with Lipschitz boundary $\partial\Omega$, $\boldsymbol{\nu}$ is the unit normal vector pointing outward $\partial\Omega$ and φ_0 is a given initial concentration. With a slight abuse of notation for the sake of compactness, we have indicated with $H'_\lambda(\varphi)$ the functional derivative of $H_\lambda(\varphi)$ with respect to φ. Observe that the equation degenerates on

the set $\{\varphi = 0, \varphi = 1\}$ but the (potential) singularity is concentrated on the set $\{\varphi = 1\}$ only. This is a non-trivial difference with respect to the well-known Cahn–Hilliard equation studied in literature (see for details [30,61]). This was also pointed out in [1] where (2.14) without the nonlocal term was analysed. More recently, a sort of relaxation of this problem has been considered in [59]. In the following, the existence of a weak solution will be proven as well as the convergence to a solution to the original problem studied in [1]. In addition, the long-term convergence of a subsequence of solutions to a stationary state will be also established.

2.2. Functional spaces and notation

For a given bounded domain $\Omega \subset \mathbb{R}^d$, $d = 1, 2, 3$, we denote with $L^p(\Omega)$, $W^{m,p}(\Omega)$, $H^m(\Omega) = W^{m,2}(\Omega)$ and $L^p(0,T;V)$ the usual Lebesgue, Sobolev and Bochner spaces, with $p \in [1,\infty]$, $m \in \mathbb{N}$ and V being a suitable (separable) real Hilbert space. Given a time interval $[0,T]$, $T > 0$, we set $\Omega_T = \Omega \times (0,T)$.

Denoting with V^* the topological dual of a given Banach (or Hilbert) space V, the inner product in V and the duality pairing between V and V^* will be indicated with the symbols $(\cdot,\cdot)_V$ and $\langle \cdot,\cdot \rangle_{V \times V^*}$, respectively. If $V = H^1(\Omega)$ then the duality pairing will be denoted by $\langle \cdot,\cdot \rangle_*$ for the ease of notation.

Symbols $C^n(\Omega)$ and $C^n(I_1, I_2)$, $n \geq 0$, indicate the spaces of C^n-functions from Ω to $\mathbb{R}$ and from intervals $I_1 \subset \mathbb{R}$ to $I_2 \subset \mathbb{R}$, respectively. Moreover, if $d = 1$, then we denote by $C^{s_1,s_2}(\Omega_T)$ the space of Hölder continuous functions from Ω_T to $\mathbb{R}$ with exponents s_1 and s_2 with respect to x and t, respectively. Also, we make use of the following notation

$$\{0 < u < 1\} = \{(\mathbf{x}, t) \in \Omega_T : 0 < u(\mathbf{x}, t) < 1\}$$

for a given measurable function $u : \Omega_T \to \mathbb{R}$.

We shall use the standard notation when dealing with Bochner spaces. Thereby, a function $u = u(\mathbf{x}, t)$ depending on space and time is considered as a function of time alone with values to a Hilbert (or Sobolev) space V, that is

$$u : [0,T] \to V. \tag{2.15}$$

With this convention, $u(t)$ and $\dot{u}(t)$ will be used instead of $u(\mathbf{x}, t)$ and $u_t(\mathbf{x}, t)$. Throughout the discussion, $C, C_1, \ldots C_n$ denote generic positive constant and when possible the numeration will help to keep track of the changes. Eventual dependencies of the constants on geometrical or physical parameters will be explicitly indicated.

2.3. Numerical setting

Let $h > 0$ be a discretization parameter and $\mathcal{T}_h$ a quasi-uniform conforming decomposition of the domain $\Omega \subset \mathbb{R}^d$, $d = 1, 2, 3$, into d-simplices K, with $h_K = \mathrm{diam}(K)$ and $h = \max_{K \in \mathcal{T}_h} h_K$. We introduce the following finite-element spaces:

$$S_h := \{v_h \in C^0(\bar{\Omega}) : v_h|_K \in \mathbb{P}_1(K), \forall K \in \mathcal{T}_h\} \subset H^1(\Omega),$$
$$S_h^+ := \{v_h \in S_h : v_h \geq 0 \text{ in } \Omega\},$$

where $\mathbb{P}_1(K)$ stands for the space of polynomials of total order 1 in K. Let J be the set of nodes of $\mathcal{T}_h$, $\{\mathbf{x}_j\}_{j\in J}$ the set of their coordinates, and $\{\phi_j\}_{j\in J}$ the Lagrangian basis functions associated with each node $j \in J$ and such that

$$\phi_j(\mathbf{x}_i) = \delta_{ij}.$$

Denoting by $\Pi_h : C^0(\bar{\Omega}) \to S_h$ the standard Lagrangian interpolation operator such that

$$\Pi_h u(\mathbf{x}_j) = u(\mathbf{x}_j) \qquad \forall j \in J,$$

we define the lumped scalar product (or discrete semi-inner product) as

$$(u, v)_h = \int_\Omega \Pi_h[u(\mathbf{x})v(\mathbf{x})]d\mathbf{x} \equiv \sum_{j\in J}(1, \phi_j)_{L^2(\Omega)}u(\mathbf{x}_j)v(\mathbf{x}_j), \tag{2.16}$$

for all $u, v \in C^0(\bar{\Omega})$. We also introduce the L^2-projection operator $P_h : L^2(\Omega) \to S_h$ and its lumped version $\hat{P}_h : L^2(\Omega) \to S_h$ defined by

$$(P_h u, v_h)_{L^2(\Omega)} = (u, v_h)_{L^2(\Omega)} \qquad \forall v_h \in S_h, \tag{2.17}$$

$$(\hat{P}_h u, v_h)_h = (u, v_h)_{L^2(\Omega)} \qquad \forall v_h \in S_h. \tag{2.18}$$

3. Existence of a weak solution

In this section we prove the existence of a weak solution to the problem (2.14). First, we introduce a suitable regularized problem in order to deal with the degeneracy set of the mobility and the singularity of the potential. For this problem we find a weak solution and provide a regularity result. Then we establish suitable *a priori* estimates which are uniform with respect to the regularization parameters. Such estimates are eventually used to pass to the limit and establish the existence of a weak solution to problem (2.14). Moreover, we will see that some additional regularity properties can be proven in the one-dimensional case.

3.1. The regularized problem

The approach extends the strategy presented in [1] (see also [30]) to account for the presence of the elastic nonlocal term. We refer to the quoted works for a complete characterization of the properties of the regularized functions. Given $\varepsilon, \delta \in (0, 1)$, we introduce a regularized mobility by setting

$$b_{\delta,\varepsilon}(r) = \begin{cases} b(\delta) & r \le \delta \\ b(r) & \delta < r < 1-\varepsilon \\ b(1-\varepsilon) & r \ge 1-\varepsilon \end{cases} \qquad \forall r \in \mathbb{R}. \tag{3.1}$$

On the other hand, to account for the singularity of the potential in $\varphi = 1$, we exploit the Lennard-Jones splitting (2.7) and define two extensions of the functions ψ_1 and ψ_2, such that

$$\psi''_{1,\varepsilon}(r) = \begin{cases} \psi''_1(1-r) & r \geq 1-\varepsilon \\ \psi''_1(r) & r < 1-\varepsilon \end{cases} \qquad \forall r \in \mathbb{R}, \tag{3.2}$$

and

$$\bar{\psi}_2(r) = \begin{cases} \psi_2(1) + \psi'_2(1)(r-1) + \dfrac{1}{2}\psi''_2(1)(r-1)^2 & r \geq 1 \\ \psi_2(r) & r \leq 1. \end{cases} \tag{3.3}$$

The regularized potential is thus defined as follows

$$\psi_\varepsilon(r) = \psi_{1,\varepsilon}(r) + \bar{\psi}_2(r). \tag{3.4}$$

Summing up, on account of (3.1), (3.4) and (2.11), we introduce the following regularized version of problem (2.14):

$$\begin{cases} \dfrac{\partial \varphi_{\delta,\varepsilon}}{\partial t} = \nabla \cdot \left[b_{\delta,\varepsilon}(\varphi_{\delta,\varepsilon}) \nabla \mu_{\delta,\varepsilon} \right] & \text{in } \Omega_T \\ \mu_{\delta,\varepsilon} = \psi'_\varepsilon(\varphi_{\delta,\varepsilon}) - \gamma^2 \Delta \varphi_{\delta,\varepsilon} + \kappa H'_\lambda(\varphi_{\delta,\varepsilon}) A^\lambda_{\delta,\varepsilon}(\varphi_{\delta,\varepsilon}) & \text{in } \Omega_T \\ \varphi_{\delta,\varepsilon}(\mathbf{x}, 0) = \varphi_0(\mathbf{x}) & \text{in } \Omega \\ \nabla \varphi_{\delta,\varepsilon} \cdot \boldsymbol{\nu} = b_{\delta,\varepsilon}(\varphi_{\delta,\varepsilon}) \nabla \mu_{\delta,\varepsilon} \cdot \boldsymbol{\nu} = 0 & \text{on } \partial\Omega \times (0,T), \end{cases} \tag{3.5}$$

where $A^\lambda_{\delta,\varepsilon}(\varphi_{\delta,\varepsilon})$ stands for

$$A^\lambda_{\delta,\varepsilon}(\varphi_{\delta,\varepsilon}) = \int_\Omega \left[H_\lambda(\varphi_{\delta,\varepsilon}) - H_\lambda(\bar{\varphi}) \right] d\mathbf{x}.$$

Problem (3.5) admits a weak solution in the following sense:

Theorem 3.1. *Let Ω be a subset of $\mathbb{R}^d$ with $\partial\Omega$ at least of class C^1, and suppose that $\varphi_0 \in H^1(\Omega)$. Then, for every $T \in (0, \infty)$ there exists a pair $(\varphi_{\delta,\varepsilon}, \mu_{\delta,\varepsilon})$ such that*

$$\varphi_{\delta,\varepsilon} \in L^\infty(0,T; H^1(\Omega)) \tag{3.6a}$$

$$\dot{\varphi}_{\delta,\varepsilon} \in L^2(0,T; (H^1(\Omega))^*) \tag{3.6b}$$

$$\mu_{\delta,\varepsilon} \in L^2(0,T; H^1(\Omega)) \tag{3.6c}$$

$$\varphi_{\delta,\varepsilon}(0) = \varphi_0 \tag{3.6d}$$

and satisfying the following mixed weak formulation

$$\begin{cases} \displaystyle\int_0^T \langle \dot{\varphi}_{\delta,\varepsilon}(t), \xi(t) \rangle_* dt + \int_0^T \int_\Omega b_{\delta,\varepsilon}(\varphi_{\delta,\varepsilon}(t)) \nabla \mu_{\delta,\varepsilon} \cdot \nabla \xi(t) d\mathbf{x} dt = 0 \\ \displaystyle\int_\Omega \mu_{\delta,\varepsilon} \phi d\mathbf{x} = \int_\Omega \psi'_\varepsilon(\varphi_{\delta,\varepsilon}) \phi d\mathbf{x} + \gamma^2 \int_\Omega \nabla \varphi_{\delta,\varepsilon} \cdot \nabla \phi d\mathbf{x} \\ + \kappa A^\lambda_{\delta,\varepsilon}(\varphi_{\delta,\varepsilon}) \displaystyle\int_\Omega H'_\lambda(\varphi_{\delta,\varepsilon}) \phi d\mathbf{x} \qquad \text{a.e. in } [0,T] \end{cases} \tag{3.7}$$

for every $\xi \in L^2(0,T; H^1(\Omega))$ and $\phi \in H^1(\Omega)$.

Proof. The proof is based on a Faedo-Galerkin approach and can be carried out following [30]. It is worth noting at this stage that the bounds of the Faedo-Galerkin sequence $\{\varphi_m\}$ easily follow from the boundedness properties of (2.11). Therefore, since standard compactness arguments entail that $\varphi_m \to \varphi_{\delta,\varepsilon}$ in $C^0([0,T];L^2(\Omega))$ and a.e. in Ω_T, and, moreover, $H_\lambda \in C^\infty(\mathbb{R}) \cap W^{1,\infty}(\mathbb{R})$, we have that

$$A_m^\lambda(\varphi_m)\int_\Omega H'_\lambda(\varphi_m)\phi_j d\mathbf{x} \to A^\lambda_{\delta,\varepsilon}(\varphi_{\delta,\varepsilon})\int_\Omega H'_\lambda(\varphi_{\delta,\varepsilon})\phi_j d\mathbf{x}, \tag{3.8}$$

as $m \to \infty$, where

$$A_m^\lambda(\varphi_m) = \int_\Omega \left[H_\lambda(\varphi_m) - H_\lambda(\bar{\varphi})\right] d\mathbf{x}. \tag{3.9}$$

Thanks to this observation we pass to the limit in the elastic contribution. Thus we can prove that the limit point actually satisfies the weak formulation (3.7). ∎

Remark 3.1. In the definition of the weak solution of the regularized problem it is essential to underline that the total mass is conserved, allowing the use of Poincaré-type inequality. More precisely, we have

$$⨍_\Omega \varphi_{\delta,\varepsilon}(t) = ⨍_\Omega \varphi_0,$$

for all $t \in [0,T]$.

Remark 3.2. Using standard elliptic regularity theory, on account of [1, Lemma 2], we can show that a weak solution to the problem (3.5), in the sense of (3.1), belongs to the space $L^2(0,T;H^3(\Omega))$. This additional regularity entails that the solution to the regularized problem satisfies the primal weak formulation

$$\begin{aligned}&\int_0^T \langle \dot{\varphi}_{\delta,\varepsilon}, \xi\rangle_* \, dt + \\ &+ \int_0^T \int_\Omega b_{\delta,\varepsilon}(\varphi_{\delta,\varepsilon})\nabla\left[\psi'_\varepsilon(\varphi_{\delta,\varepsilon}) - \gamma^2\Delta\varphi_{\delta,\varepsilon} + \kappa A^\lambda_{\delta,\varepsilon}(\varphi_{\delta,\varepsilon})H'_\lambda(\varphi_{\delta,\varepsilon})\right]\cdot\nabla\xi \, d\mathbf{x}dt = 0\end{aligned} \tag{3.10}$$

for every $\xi \in L^2(0,T;H^1(\Omega))$, with $\varphi_{\delta,\varepsilon}(0) = \phi_0$, where the equations for $\varphi_{\delta,\varepsilon}$ and $\mu_{\delta,\varepsilon}$ are not decoupled.

3.2. *A priori* energy and entropy estimates

Here we prove suitable *a priori* bounds on a solution to the approximate problem which are uniform with respect to δ and ε. Such bounds will be essential to establish the existence of a weak solution to the original problem. Following similar arguments as in [1, 30], the following lemma can be proved:

Lemma 3.1. *Given $\varphi_0 \in H^1(\Omega)$, $0 \le \varphi_0 < 1$, there exists $\varepsilon_0 < 1$ such that for all $0 < \varepsilon \le \varepsilon_0$ and $\delta \in (0,1)$ the following estimate holds*

$$\begin{aligned} &\operatorname{ess\,sup}_{[0,T]} \left\{ \int_\Omega \left[\frac{\gamma^2}{2} |\nabla \varphi_{\delta,\varepsilon}|^2 + \psi_\varepsilon(\varphi_{\delta,\varepsilon}) \right] d\mathbf{x} + \frac{\kappa}{2} \left[A^\lambda_{\delta,\varepsilon}(\varphi_{\delta,\varepsilon}) \right]^2 \right\} \\ &+ \int_0^T \int_\Omega b_{\delta,\varepsilon}(\varphi_{\delta,\varepsilon}) |\nabla \mu_{\delta,\varepsilon}|^2 d\mathbf{x} dt \le C, \end{aligned} \tag{3.11}$$

with a constant C independent of δ and ε.

A further basic *a priori* bound is concerned with the entropy function $\Phi_{\delta,\varepsilon}$ defined by

$$\Phi_{\delta,\varepsilon}(r) = \int_R^r \Psi_{\delta,\varepsilon}(s) ds, \tag{3.12}$$

where

$$\Psi_{\delta,\varepsilon}(r) = \int_R^r \frac{ds}{b_{\delta,\varepsilon}(s)} \tag{3.13}$$

and $\Phi_{\delta,\varepsilon}(R) = \Psi_{\delta,\varepsilon}(R) = 0$ with $0 < R < 1$. Observe that

$$\Phi''_{\delta,\varepsilon}(r) = \Psi'_{\delta,\varepsilon}(r) = \frac{1}{b_{\delta,\varepsilon}(r)} \tag{3.14}$$

and

$$\Psi_{\delta,\varepsilon}(r) \le 0 \qquad \text{for } r < R \tag{3.15a}$$

$$\Phi_{\delta,\varepsilon}(r) \ge 0 \qquad \forall r \in \mathbb{R}. \tag{3.15b}$$

Moreover, we set

$$\Phi(r) = \lim_{\delta \to 0, \varepsilon \to 0} \Phi_{\delta,\varepsilon}(r), \qquad \Psi(r) = \lim_{\delta \to 0, \varepsilon \to 0} \Psi_{\delta,\varepsilon}(r)$$

and we observe that

$$\Phi_{\delta,\varepsilon}(r) \le \Phi(r) \qquad 0 \le r \le 1. \tag{3.16}$$

A straightforward computation (see (2.5)) gives

$$\Psi(r) = \frac{1}{1-r} - \ln(1-r) + \ln r - C_1 \tag{3.17}$$

$$\Phi(r) = r \ln r - r \ln(1-r) - C_1 r + C_2, \tag{3.18}$$

being C_1, C_2 positive constants.
On account of the above considerations, the following entropy estimate can be proved:

Lemma 3.2. *If $0 \le \varphi_0 < 1$, there exists $\varepsilon_0 > 0$ such that, for all $0 < \varepsilon \le \varepsilon_0$ and $\delta > 0$, the following estimate holds with a constant C independent of δ and ε:*

$$\int_\Omega \Phi_{\delta,\varepsilon}(\varphi_{\delta,\varepsilon})\, d\mathbf{x} + \int_0^T \int_\Omega \psi''_{1,\varepsilon}(\varphi_{\delta,\varepsilon}) |\nabla \varphi_{\delta,\varepsilon}|^2\, d\mathbf{x} dt + \gamma^2 \int_0^T \int_\Omega |\Delta \varphi_{\delta,\varepsilon}|^2\, d\mathbf{x} dt \le C, \tag{3.19}$$

for almost all $t \in [0,T]$.

This estimate can be formally obtained noticing that $\Psi_{\delta,\varepsilon}(\varphi_{\delta,\varepsilon})$ is an admissible test function for the primal weak formulation (3.10). Treating the temporal derivative as in the proof of (3.11) [1, 30], integrating by parts the term containing the Laplacian, and using (3.16)-(3.18), together with the terms estimated by (3.11), we obtain the desired result. As in [1], in order to control the term with ψ_2'', we employ a Sobolev inequality. Moreover, uniform boundedness of $(A^\lambda H_\lambda')'$ comes into play.

In the next subsections we will use (3.11) and (3.19) to pass to the limit as $\delta, \varepsilon \to 0$ in problem (3.5) and prove existence of a weak solution to problem (2.14). The case $d = 1$ is treated separately from $d = 2, 3$, since in the latter cases we cannot establish the uniform convergence of the regularized solutions. Moreover, if $d = 1$ then we can show that the weak solution possesses further regularity properties.

3.3. Passage to the limit in the case d = 1

The proof follows [1] and [8], with suitable modifications due to the presence of the non-local term and the use of a dual weak formulation for the original problem. As in the regularized problem, the weak solution defined in the following Theorem 3.2 (and Theorem 3.3 for the case $d = 2, 3$) fulfills the mass conservation (see Remark 3.1).

Theorem 3.2. *Let $d = 1$ and $\varphi_0 \in H^1(\Omega)$ with $0 \le \varphi_0 < 1$. Then, there exist a subsequence of $(\varphi_{\delta,\varepsilon}, \mu_{\delta,\varepsilon})$ and functions*

$$\begin{aligned} \varphi &\in L^\infty(0,T;H^1(\Omega)) \cap C^{\frac{1}{2},\frac{1}{8}}(\bar{\Omega}_T) \\ \dot{\varphi} &\in L^2(0,T;(H^1(\Omega))^*) \\ \mu &\in L^2_{loc}(\{0<\varphi<1\}) \\ \frac{\partial \mu}{\partial x} &\in L^2_{loc}(\{0<\varphi<1\}), \end{aligned}$$

such that, as $\delta, \varepsilon \to 0$ along a suitable subsequence,

$$\varphi_{\delta,\varepsilon} \overset{*}{\rightharpoonup} \varphi \qquad \text{in } L^\infty(0,T;H^1(\Omega)) \tag{3.20a}$$

$$\varphi_{\delta,\varepsilon} \to \varphi \qquad \text{uniformly on } \bar{\Omega}_T \tag{3.20b}$$

$$\mu_{\delta,\varepsilon} \rightharpoonup \mu \qquad \text{in } L^2_{loc}(\{0<\varphi<1\}) \tag{3.20c}$$

$$\frac{\partial \mu_{\delta,\varepsilon}}{\partial x} \rightharpoonup \frac{\partial \mu}{\partial x} \qquad \text{in } L^2_{loc}(\{0<\varphi<1\}). \tag{3.20d}$$

Moreover, $0 \le \varphi < 1$ almost everywhere in $\bar{\Omega}_T$ and the limit point (φ, μ) satisfies the weak formulation of problem (2.14) in the following sense:

$$\begin{cases} \displaystyle\int_0^T \langle \dot{\varphi}, \xi \rangle_* dt + \int_{\{0<\varphi<1\}} b(\varphi) \frac{\partial \mu}{\partial x} \frac{\partial \xi}{\partial x}\, dx dt = 0 \\ \displaystyle\int_{\{0<\varphi<1\}} \mu\phi\, dx dt = \int_{\{0<\varphi<1\}} \psi'(\varphi)\phi\, dx dt + \gamma^2 \int_{\{0<\varphi<1\}} \frac{\partial \varphi}{\partial x} \frac{\partial \phi}{\partial x}\, dx dt \\ \qquad\qquad + \kappa \displaystyle\int_{\{0<\varphi<1\}} A^\lambda(\varphi) H_\lambda'(\varphi)\phi\, dx dt \end{cases} \tag{3.21}$$

for all $\xi, \phi \in L^2(0,T;H^1(\Omega))$*, with* $\varphi(0) = \varphi_0$.

Proof. The proof consists of four steps.

(1) *Proof of* (3.20a) *and* (3.20b)
Weak-$*$ convergence of $\varphi_{\delta,\varepsilon}$ with respect to the $L^\infty(0,T;H^1(\Omega))$-norm follows directly from energy estimate (3.11), which entails a bound for $\|\nabla\varphi_{\delta,\varepsilon}(t)\|_{L^2(\Omega)}$. Then, on account of the mass conservation, we get the desired convergence. If $d = 1$ then we can use the embedding of $H^1(\Omega)$ in $L^\infty(\Omega)$, together with the Poincaré-Wirtinger inequality and (3.11) to obtain a uniform bound in $\bar{\Omega}$:

$$\begin{aligned}\|\varphi_{\delta,\varepsilon}(t)\|^2_{L^\infty(\Omega)} &\le C^*\|\varphi_{\delta,\varepsilon}(t)\|^2_{H^1(\Omega)}\\ &\le C^*(1+C_P^2)\|\nabla\varphi_{\delta,\varepsilon}(t)\|^2_{L^2(\Omega)} \le CC^*(1+C_P^2).\end{aligned}$$

Therefore, we have

$$|\varphi_{\delta,\varepsilon}(x,t)| \le \sqrt{CC^*(1+C_P^2)},$$

where all constants are independent of δ and ε, showing that $\{\varphi_{\delta,\varepsilon}\}$ is uniformly bounded on $\bar{\Omega}_T$. Following [8, Lemma 2.1] we can also prove that there exists an upper bound of $\{\varphi_{\delta,\varepsilon}\}$ in the $C^{\frac{1}{2},\frac{1}{8}}(\bar{\Omega}_T)$-norm, meaning that

$$\begin{aligned}|\varphi_{\delta,\varepsilon}(x_2,t) - \varphi_{\delta,\varepsilon}(x_1,t)| &\le K_1|x_2 - x_1|^{\frac{1}{2}}\\ |\varphi_{\delta,\varepsilon}(x,t_2) - \varphi_{\delta,\varepsilon}(x,t_1)| &\le K_1|t_2 - t_1|^{\frac{1}{8}},\end{aligned}$$

with $K_1, K_2 > 0$ uniform in the regularization parameters. First relation follows actually from Morrey's inequality

$$\|v\|_{C^{0,\alpha}(\bar{\Omega})} \le C_M(\Omega,d,p)\|v\|_{W^{1,p}(\Omega)} \quad \text{for all } v \in W^{1,p}(\Omega),$$

with $d = 1$, $p = 2$ and therefore $\alpha = \frac{1}{2}$. Thus, functions $\varphi_{\delta,\varepsilon}$ are all Hölder continuous with the same constants so that $\{\varphi_{\delta,\varepsilon}\}$ is a equi-continuous bounded family of functions. From the Ascoli-Arzelà theorem we obtain (3.20b).

(2) *Proof of* $0 \le \varphi < 1$
The proof can be taken verbatim from [1].

(3) *Proof of* (3.20c) *and* (3.20d)
This proof stems by the compactness result in Banach spaces. The difficult part is to show the boundedness of $\mu_{\delta,\varepsilon}$ and $\frac{\partial\mu_{\delta,\varepsilon}}{\partial x}$ in the space $L^2_{loc}(\{0<\varphi<1\})$. For this purpose, for any $\eta > 0$ we set

$$\begin{aligned}D^+_\eta &= \{(x,t) \in \bar{\Omega}_T : \eta < \varphi(x,t) < 1\}\\ D^+_\eta(t) &= \{x \in \bar{\Omega} : \eta < \varphi(x,t) < 1\},\end{aligned}$$

and we introduce a cutoff function $\theta_\eta \in C^\infty_0(D^+_{\frac{\eta}{4}})$ such that $\theta_\eta(\cdot,t) \equiv 1$ on $D^+_{\frac{\eta}{2}}(t)$ and $0 \le \theta_\eta(\cdot,t) \le 1$. Observe that $\phi = \theta^2_\eta\mu_{\delta,\varepsilon} \in H^1(\Omega)$ is a valid test function to

take in (3.7). Recalling that θ_η is compactly supported on $S := D^+_{\frac{\eta}{4}}$, we get

$$\int_0^T \int_\Omega \theta_\eta^2 \mu_{\delta,\varepsilon}^2 \, dx = \int_S \psi'_\varepsilon(\varphi_{\delta,\varepsilon}) \theta_\eta^2 \mu_{\delta,\varepsilon} \, dx + \gamma^2 \int_S \frac{\partial \varphi_{\delta,\varepsilon}}{\partial x} \frac{\partial}{\partial x}(\theta_\eta^2 \mu_{\delta,\varepsilon}) \, dx + \kappa \int_S A^\lambda_{\delta,\varepsilon}(\varphi_{\delta,\varepsilon}) H'_\lambda(\varphi_{\delta,\varepsilon}) \theta_\eta^2 \mu_{\delta,\varepsilon} \, dx.$$

Let us consider the three terms on the right hand side of the latter equation, separately. The first and the second integrals can be bounded using (3.11) as in [1, 30], obtaining

$$\int_S \psi'_\varepsilon(\varphi_{\delta,\varepsilon}) \theta_\eta^2 \mu_{\delta,\varepsilon} \, dx \le C_1 \|\theta_\eta \mu_{\delta,\varepsilon}\|_{L^2(S)} \tag{3.22}$$

$$\int_S \frac{\partial \varphi_{\delta,\varepsilon}}{\partial x} \frac{\partial}{\partial x}(\theta_\eta^2 \mu_{\delta,\varepsilon}) dx \le 2C_2 C \eta^{-2} \|\theta_\eta \mu_{\delta,\varepsilon}\|_{L^2(S)} + C_2 \left\| \frac{\partial \mu_{\delta,\varepsilon}}{\partial x} \right\|_{L^2(S)}. \tag{3.23}$$

For the third term we proceed once again as in [1], exploiting the fact that the non–locality is here uniformly bounded:

$$\int_S A^\lambda_{\delta,\varepsilon}(\varphi_{\delta,\varepsilon}) H'_\lambda(\varphi_{\delta,\varepsilon}) \theta_\eta^2 \mu_{\delta,\varepsilon} dx \le C_3 \|\theta_\eta \mu_{\delta,\varepsilon}\|_{L^2(S)}. \tag{3.24}$$

Adding together (3.22)-(3.24), and renaming the constants to ease the notation, we get

$$\int_0^T \int_\Omega \theta_\eta^2 \mu_{\delta,\varepsilon}^2 dx \le C \left(1 + \eta^{-2}\right) \|\theta_\eta \mu_{\delta,\varepsilon}\|_{L^2(S)} + C \left\| \frac{\partial \mu_{\delta,\varepsilon}}{\partial x} \right\|_{L^2(S)}. \tag{3.25}$$

Following once again [1], we end up with

$$\|\mu_{\delta,\varepsilon}\|_{L^2(0,T;H^1(D^+_{\frac{\eta}{4}}(t)))} \le C + C\eta^{-4}, \tag{3.26}$$

for every fixed $\eta > 0$. This bound holds for any compact subset of the set $D_0^+ \equiv \{0 < \varphi < 1\}$ and implies the boundedness of $\{\mu_{\delta,\varepsilon}\}$ in $L^2_{\text{loc}}(\{0 < \varphi < 1\})$. From standard compactness results, (3.20c)-(3.20d) follow. Moreover, from boundedness of $\{\varphi_{\delta,\varepsilon}\}$ on Ω_T and (3.11) we get that

$$b(\varphi_{\delta,\varepsilon}) \frac{\partial \mu_{\delta,\varepsilon}}{\partial x} \in L^2(\Omega_T)$$

and this entails, by comparison in the first equation of (3.7), the weak convergence

$$\dot{\varphi}_{\delta,\varepsilon} \rightharpoonup \dot{\varphi} \qquad \text{in } L^2(0,T;(H^1(\Omega))^*). \tag{3.27}$$

(4) *The limit point satisfies the weak formulation and the initial condition*
The above ingredients allow us to show the existence of a suitable subsequence of the approximating pair $(\varphi_{\delta,\varepsilon}, \mu_{\delta,\varepsilon})$ converging to a solution of (3.21), up to a subsequence. Once again, the proof can be adapted from [1].

■

3.4. Passage to the limit in the cases d = 2 and d = 3

In this case we are unable to prove uniform convergence of the regularized solution. Therefore $\nabla\mu_{\delta,\varepsilon}$ might not have a (weak) limit in $L^2(\Omega_T)$. However, (3.19) helps us to identify a class of approximating weak solutions for which we can take the limit as $\delta, \varepsilon \to 0$, up to a suitable subsequence. This requires a convenient reformulation of the regularized problem. Recalling (2.10), we introduce the regularized flux function $\mathbf{J}_{\delta,\varepsilon}$ (see (3.1)), that is,

$$\begin{aligned}\mathbf{J}_{\delta,\varepsilon} &= -b_{\delta,\varepsilon}(\varphi_{\delta,\varepsilon})\nabla\mu_{\delta,\varepsilon}\\ &= -b_{\delta,\varepsilon}(\varphi_{\delta,\varepsilon})\nabla\left[\psi'_\varepsilon(\varphi_{\delta,\varepsilon}) - \gamma\Delta\varphi_{\delta,\varepsilon} + \kappa A^\lambda_{\delta,\varepsilon}(\varphi_{\delta,\varepsilon})H'_\lambda(\varphi_{\delta,\varepsilon})\right]\end{aligned} \tag{3.28}$$

and set

$$Z(\varphi,t) = \frac{\delta\left[A^\lambda(\varphi)H'_\lambda(\varphi)\right]}{\delta\varphi}.$$

The proof of the theorem essentially follows [30, Theorem 1] (see also [36, Theorem 1.2] and [1, Theorem 3]), with all the necessary modifications.

Theorem 3.3. *Let $d = 2, 3$ and $\varphi_0 \in H^1(\Omega)$ with $0 \le \varphi_0 < 1$ almost everywhere in Ω. Then, there exist a subsequence of $(\varphi_{\delta,\varepsilon}, \mathbf{J}_{\delta,\varepsilon})$ and functions*

$$\begin{aligned}&\varphi \in L^\infty(0,T;H^1(\Omega)) \cap L^2(0,T;H^2(\Omega))\\ &\dot\varphi \in L^2(0;T;(H^1(\Omega))^*)\\ &\mathbf{J} \in L^2(\Omega_T,\mathbb{R}^d)\end{aligned}$$

such that, as $\delta, \varepsilon \to 0$ along a suitable subsequence,

$$\varphi_{\delta,\varepsilon} \overset{*}{\rightharpoonup} \varphi \qquad \text{in } L^\infty(0,T;H^1(\Omega)) \tag{3.29a}$$

$$\dot\varphi_{\delta,\varepsilon} \rightharpoonup \dot\varphi \qquad \text{in } L^2(0,T;(H^1(\Omega))^*) \tag{3.29b}$$

$$\Delta\varphi_{\delta,\varepsilon} \rightharpoonup \Delta\varphi \qquad \text{in } L^2(\Omega_T) \tag{3.29c}$$

$$\mathbf{J}_{\delta,\varepsilon} \rightharpoonup \mathbf{J} \qquad \text{in } L^2(\Omega_T). \tag{3.29d}$$

Moreover, $0 \le \varphi < 1$ almost everywhere in $\bar\Omega_T$ and the limit point $(\varphi, \mathbf{J})$ satisfies the following weak formulation of problem (2.14):

$$\begin{cases}\displaystyle\int_0^T \langle\dot\varphi,\xi\rangle_* dt = \int_0^T\int_\Omega \mathbf{J}\cdot\nabla\xi d\mathbf{x}dt\\ \displaystyle\int_0^T\int_\Omega \mathbf{J}\cdot\boldsymbol{\eta}d\mathbf{x}dt = -\int_0^T\int_\Omega \gamma^2\Delta\varphi\nabla\cdot[b(\varphi)\boldsymbol{\eta}]\,d\mathbf{x}dt\\ \qquad\qquad\qquad\qquad -\displaystyle\int_0^T\int_\Omega b(\varphi)\psi''(\varphi)\nabla\varphi\cdot\boldsymbol{\eta}d\mathbf{x}dt\\ \qquad\qquad\qquad\qquad -\displaystyle\int_0^T\int_\Omega \kappa b(\varphi)Z(\varphi)\nabla\varphi\cdot\boldsymbol{\eta}d\mathbf{x}dt\end{cases} \tag{3.30}$$

for every $\xi \in L^2(0,T;H^1(\Omega))$, $\boldsymbol{\eta} \in L^2(0,T;H^1(\Omega,\mathbb{R}^d)) \cap L^\infty(\Omega_T,\mathbb{R}^d)$ *with* $\boldsymbol{\eta}\cdot\boldsymbol{\nu}=0$ *almost everywhere on* $\partial\Omega\times(0,T)$, $\varphi(0)=\varphi_0$ *almost everywhere in* Ω, *and* $\nabla\varphi\cdot\boldsymbol{\nu}=0$ *almost everywhere on* $\partial\Omega$.

Proof. The proof consists of several steps.

(1) *Proof of* (3.29a)-(3.29d)
First of all we notice that (3.29c) follows from (3.19). Standard elliptic regularity theory yields $\varphi_{\delta,\varepsilon} \in L^2(0,T;H^2(\Omega))$. Moreover, on account of (3.1), we have that (3.11) entails (3.29d). This also implies (3.29b) thanks to weak formulation (3.7). Eventually, since

$$L^\infty(0,T;H^1(\Omega)) \cap H^1(0,T;(H^1(\Omega))^*) \cap L^2(0,T;H^2(\Omega))$$

is compactly embedded in

$$C^0([0,T];L^6(\Omega)) \cap L^2(0,T;H^1(\Omega)) \cap L^2(0,T;C^0(\bar{\Omega}_T)), \tag{3.31}$$

we have (3.29a). In particular, the last space in (3.31) follows from the Rellich-Kondrachov theorem, thanks to the H^2-regularity, and interpolation in Bochner spaces (see [63]). Moreover, this convergence also ensures that $\varphi(0)=\varphi_0$ almost everywhere, since $\varphi_0 \in H^1(\Omega)$.

(2) *Proof of* $0 \le \varphi < 1$
The proof can be taken from [1].

(3) *The limit point satisfies the weak formulation*
We now prove that the limit point $(\varphi, \mathbf{J})$ satisfies (3.30). The first equation can be easily identified passing to the limit as $\delta,\varepsilon \to 0$ in the first equation of (3.7) and exploiting weak convergences (3.29b) and (3.29d). We also have $\varphi_{\delta,\varepsilon} \in L^2(0,T;H^3(\Omega))$. Hence we can multiply $\mathbf{J}_{\delta,\varepsilon}$ by a function $\boldsymbol{\eta} \in L^2(0,T;H^1(\Omega,\mathbb{R}^d)) \cap L^\infty(\Omega_T,\mathbb{R}^d)$ satisfying $\boldsymbol{\eta}\cdot\boldsymbol{\nu}=0$ almost everywhere on $\partial\Omega\times(0,T)$ and integrate over Ω_T. This gives

$$\int_0^T \int_\Omega \mathbf{J}_{\delta,\varepsilon}\cdot\boldsymbol{\eta}\,d\mathbf{x}dt = \\ -\int_T^0 \int_\Omega b_{\delta,\varepsilon}(\varphi_{\delta,\varepsilon})\nabla\left[\psi_\varepsilon'(\varphi_{\delta,\varepsilon}) - \gamma\Delta\varphi_{\delta,\varepsilon} + \kappa A^\lambda_{\delta,\varepsilon}(\varphi_{\delta,\varepsilon})H_\lambda'(\varphi_{\delta,\varepsilon})\right]\cdot\boldsymbol{\eta}\,d\mathbf{x}dt,$$

and integrating by parts on the right hand side, we obtain

$$\begin{aligned}\int_0^T \int_\Omega \mathbf{J}_{\delta,\varepsilon}\cdot\boldsymbol{\eta}\,d\mathbf{x}dt = &-\int_0^T \int_\Omega \gamma^2\Delta\varphi_{\delta,\varepsilon}\nabla\cdot\left[b_{\delta,\varepsilon}(\varphi_{\delta,\varepsilon})\boldsymbol{\eta}\right]d\mathbf{x}dt \\ &-\int_0^T \int_\Omega b_{\delta,\varepsilon}(\varphi_{\delta,\varepsilon})\psi_\varepsilon''(\varphi_{\delta,\varepsilon})\nabla\varphi_{\delta,\varepsilon}\cdot\boldsymbol{\eta}\,d\mathbf{x}dt \\ &-\int_0^T \int_\Omega \kappa b_{\delta,\varepsilon}(\varphi_{\delta,\varepsilon})Z_{\delta,\varepsilon}(\varphi_{\delta,\varepsilon})\nabla\varphi_{\delta,\varepsilon}\cdot\boldsymbol{\eta}\,d\mathbf{x}dt,\end{aligned} \tag{3.32}$$

where $Z_{\delta,\varepsilon}(\varphi_{\delta,\varepsilon})$ is given by

$$Z_{\delta,\varepsilon}(\varphi_{\delta,\varepsilon}) = \frac{\delta\left[A^{\lambda}_{\delta,\varepsilon}(\varphi_{\delta,\varepsilon})H'_{\lambda}(\varphi_{\delta,\varepsilon})\right]}{\delta\varphi_{\delta,\varepsilon}}. \tag{3.33}$$

The left-hand side of (3.32) converges to the first term in the second equation of (3.30) thanks to weak convergence (3.29d). The first and the second integral on the right-hand side can be proved to converge to the corresponding terms in (3.30) using already established results in [1, 30]. As for the third term in the right-hand side, we know that $b_{\delta,\varepsilon}(\varphi_{\delta,\varepsilon}) \to b(\varphi)$ almost everywhere in Ω_T, but since $b(\varphi)$ is uniformly bounded thanks to (3.31), we also have convergence in L^2. Observe now that calculating the functional derivative (see (3.33))

$$Z_{\delta,\varepsilon}(\varphi_{\delta,\varepsilon}) = (A^{\lambda}_{\delta,\varepsilon})'(\varphi_{\delta,\varepsilon})H'_{\lambda}(\varphi_{\delta,\varepsilon}) + A^{\lambda}_{\delta,\varepsilon}(\varphi_{\delta,\varepsilon})H''_{\lambda}(\varphi_{\delta,\varepsilon})$$

and recalling the regularity and boundedness properties of H_λ, we can apply the dominated convergence theorem and obtain

$$Z_{\delta,\varepsilon}(\varphi_{\delta,\varepsilon})b_{\delta,\varepsilon}(\varphi_{\delta,\varepsilon}) \to Z(\varphi)b(\varphi) \qquad \text{in } L^2(\Omega_T). \tag{3.34}$$

Using (3.29a) once again, together with (3.34) and the fact that $\boldsymbol{\eta}$ belongs to the space $L^\infty(\Omega_T, \mathbb{R}^d)$, we can pass to the limit as $\delta, \varepsilon \to 0$ in the third term on the right hand side of (3.32). This concludes the proof, having shown that the limit point is a solution to (3.30).

■

4. Continuous Galerkin-Finite Element approximation and numerical simulations

We study now the finite element and time discretization of problem (2.14). The entropy estimate (3.19), which guarantees the positivity of the solution, is not straightforwardly available at the discrete level, thereby it will be imposed as a constraint through a variational inequality [1, 7].

4.1. Discrete problem with explicit treatment of the nonlocal term

At the continuum level, the weak solution φ of problem (2.14) satisfies the positivity property $\varphi \in [0, 1)$ almost everywhere in Ω_T, where $\varphi \geq 0$ follows from entropy estimate (3.19), and $\varphi < 1$ follows from energy estimate (3.11). At the discrete level this is no longer true: given $v_h \in S_h$ we have

$$\nabla[P_h(\Psi(v_h))] \neq \frac{1}{b(v_h)}\nabla v_h,$$

because of the definition of function Ψ given in (3.17) and the presence of the logarithmic term (the logarithm of a $\mathbb{P}_1$ function is not a $\mathbb{P}_1$ function). In [37], a suitable approximation of the mobility $\bar{b}$ has been introduced such that $\bar{b}(v_h)\nabla[P_h(\Psi(v_h))] = \nabla v_h$, which consists of an harmonic average of the mobility on a structured mesh [1]. Due to the constraint of working with structured meshes, the aforementioned approximation is not feasible in applications. The positivity property is here imposed as a constraint through a variational inequality. In order to show the potential of the model, we present here a simple numerical scheme which relies on the convex splitting (2.7) of the potential ψ. For what concerns the nonlinearity associated to the nonlocal term, which we rename as

$$\mathcal{N}(\varphi) := \kappa \left[A^\lambda(\varphi)\right]^2,$$

where κ and $A^\lambda(\varphi)$ are defined in (2.12) and (2.13). We remark that it is difficult to impose explicitly its convex splitting, which would depend on the *a priori* unknown sign of $A^\lambda(\varphi)$. Therefore, for the sake of simplicity, we prefer to treat explicitly the nonlocal term, postponing the design of a more refined numerical method to a later work.

Denoting the time step with $\triangle t = T/N$, for a $N \in \mathbb{N}$, and $t_n = n\triangle t, n = 1, \dots, N$, we consider the following fully discretized semi-implicit approximation scheme with explicit treatment of the nonlocal term: *for* $n = 1, \dots, N$, *given* $\varphi_h^{n-1} \in S_h^+$, *find* $(\varphi_h^n, \mu_h^n) \in S_h^+ \times S_h$ *such that, for all* $(\xi, \phi) \in S_h \times S_h^+$,

$$\begin{cases} \left(\dfrac{\varphi_h^n - \varphi_h^{n-1}}{\triangle t}, \xi\right)_h + \left(b(\varphi_h^{n-1})\nabla\mu_h^n, \nabla\xi\right)_{L^2(\Omega)} = 0 \\ \gamma^2 \left(\nabla\varphi_h^n, \nabla(\phi - \varphi_h^n)\right)_{L^2(\Omega)} + \left(\psi_1'(\varphi_h^n), \phi - \varphi_h^n\right)_h \\ \geq \left(\mu_h^n - \psi_2'(\varphi_h^{n-1}) - \mathcal{N}'(\varphi_h^{n-1}), \phi - \varphi_h^n\right)_h. \end{cases} \tag{4.1}$$

starting from a datum $\varphi_0 \in H^1(\Omega)$ and $\varphi_h^0 = \Pi_h\varphi_0$ (if $d = 1$), $\varphi_h^0 = \hat{P}_h\varphi_0$ (if $d = 2, 3$), with $0 \leq \varphi_h^0 < 1$. Defining the discrete energy functional $F_h : S_h \to \mathbb{R}^+$ as

$$F_h[\varphi_h^n] = \int_\Omega \left[\frac{\gamma^2}{2}|\nabla\varphi_h^n|^2 + \psi_1(\varphi_h^n) + \chi_{\mathbb{R}^+}(\varphi_h^n)\right] d\mathbf{x}, \tag{4.2}$$

where $\chi_{\mathbb{R}^+}(\cdot)$ is the characteristic function of the closed and convex set $\mathbb{R}^+$, and endowing S_h with the lumped scalar product (2.16), the variational inequality can be written in the following way:

$$\left(\mu_h^n - \psi_2'(\varphi_h^{n-1}) - \mathcal{N}'(\varphi_h^{n-1}), \phi - \varphi_h^n\right)_h + F_h[\varphi_h^n] \leq F_h[\phi] \qquad \forall \phi \in S_h^+, \tag{4.3}$$

which is equivalent to

$$\mu_h^n - \psi_2'(\varphi_h^{n-1}) - \mathcal{N}'(\varphi_h^{n-1}) \in \partial F_h[\varphi_h^n], \tag{4.4}$$

where $\partial F_h(\varphi_h^n)$ is the subdifferential of the convex and lower-semicontinuous function F_h. This formulation represents the generalized discrete analogous of the subdifferential

approach to the standard Cahn–Hilliard equation with constraints introduced in [42]. The lack of uniqueness of the solution of the continuous problem may lead to nonphysical discrete solutions with fixed support, but can be addressed thanks to the introduction of the discrete semi-inner product (2.16) and a careful subdivision of the nodes of partition $\mathcal{T}_h$ [7]. In particular, $\mathcal{T}_h$ is subdivided into elements on which $\varphi_h^{n-1} = 0$ and elements on which $\varphi_h^{n-1} \neq 0$. Given $r_h \in S_h^+$ with $\fint_\Omega r_h \in (0,1)$, we define the set of *passive nodes* $J_0(r_h) \subset J$ by

$$j \in J_0(r_h) \Leftrightarrow \hat{P}_h r_h(\mathbf{x}_j) = 0 \Leftrightarrow (r_h, \phi_j)_{L^2(\Omega)} = 0. \tag{4.5}$$

The nodes in the set

$$J_+(r_h) = J \setminus J_0(r_h)$$

are called *active nodes* and they can be partitioned into mutually disjoint and maximally connected subsets $I_m(r_h)$ such that

$$J_+(r_h) = \bigcup_{m=1}^{M} I_m(r_h),$$

for $M \geq 1$. See [7] for further details. Defining

$$\Sigma_m(r_h) = \sum_{j \in I_m(r_h)} \phi_j,$$

we note that $\Sigma_m(r_h) \equiv 1$ on each element on which $r_h \neq 0$, since all the vertices of this element belong to the same $I_m(r_h)$. Observe that there are also elements on which $r_h \equiv 0$ but still $\Sigma_m(r_h) \equiv 1$. Hence, on each element $K \in \mathcal{T}_h$, we have that $r_h \equiv 0$ or $\Sigma_m(r_h) \equiv 1$ for some m, except for those elements on which both $r_h \equiv 0$ and $\Sigma_m(r_h) \equiv 1$. Moreover we define the sets

$$\Omega_m(r_h) = \left\{ \bigcup_{K \in \mathcal{T}_h} \bar{K} : \Sigma_m(r_h)(\mathbf{x}) = 1, \forall \mathbf{x} \in K \right\}$$

that are the union of the maximally connected elements on which $r_h \neq 0$, or $r_h \equiv 0$ and the indexes of the vertices of the elements belong to $I_m(r_h)$ for a given m. These assumptions, together with the ideas introduced in [1], allow to prove existence in $S_h^+ \times S_h$ of the solution of a regularized version of (4.1). Moreover, the regularized concentration $\varphi_{h,\varepsilon}^n$ is unique without restrictions on S_h^+, while $\mu_{h,\varepsilon}^n$ is unique on $\Omega_m(\varphi_h^{n-1})$ for $m = 1, \ldots, M$ and $n = 1 \ldots, N$. The proof can be adapted from [1, Theorem 4], treating $\psi_2 + \mathcal{N}$ explicitly. Accordingly, it is also possible to produce stability bounds for the regularized solution, which lead to convergence in S_h^+ of $\varphi_{h,\varepsilon}^n$, as $\varepsilon \to 0$, to the solution φ_h^n of (4.1). As for $\mu_{h,\varepsilon}^n$, denoting with $\Omega_{m,*}(\varphi_h^{n-1})$ the set of those elements of $\Omega_m(\varphi_h^{n-1})$ on which $\varphi_h^{n-1} \neq 0$, convergence to the solution μ_h^n of (4.1) on the set $\Omega_{m,*}(\varphi_h^{n-1})$ can be also proved. The well posedness of (4.1) follows.

4.2. Numerical algorithm

We now consider a procedure for solving the variational inequality at each time step in the problem (4.1). This is based on the general splitting algorithm proposed by Barrett *et al.* in [7] (see also [6, 24, 50] for further applications with different kinds of mobility). For n fixed, we first multiply the variational inequality in (4.1) by a relaxation parameter $\rho > 0$ and we add the term

$$\left(\varphi_h^n, \phi - \varphi_h^n\right)_h$$

to both sides, obtaining

$$\begin{aligned}&\left(\varphi_h^n, \phi - \varphi_h^n\right)_h + \rho\gamma^2 \left(\nabla\varphi_h^n, \nabla(\phi - \varphi_h^n)\right)_{L^2(\Omega)} + \rho \left(\psi_1'(\varphi_h^n), \phi - \varphi_h^n\right)_h \\ &\geq \left(\varphi_h^n, \phi - \varphi_h^n\right)_h + \rho \left(\mu_h^n - \psi_2'(\varphi_h^{n-1}) - \mathcal{N}'(\varphi_h^{n-1}), \phi - \varphi_h^n\right)_h . \end{aligned} \tag{4.6}$$

Defining the function Z_h^n in such a way that

$$\left(Z_h^n, \phi\right)_h = \left(\varphi_h^n, \phi\right)_h + \rho \left(\mu_h^n - \psi_2'(\varphi_h^{n-1}) - \mathcal{N}'(\varphi_h^{n-1}), \phi\right)_h - \rho\gamma^2 \left(\nabla\varphi_h^n, \nabla\phi\right)_{L^2(\Omega)} , \tag{4.7}$$

inequality (4.6) becomes

$$\left(\varphi_h^n, \phi - \varphi_h^n\right)_h + \rho \left(\psi_1'(\varphi_h^n), \phi - \varphi_h^n\right)_h \geq \left(Z_h^n, \phi - \varphi_h^n\right)_h . \tag{4.8}$$

Due to the presence of the lumped scalar product, and the fact that the elliptic terms are contained in the vector Z_h^n, inequality (4.8) is scalar and must be satisfied on each node separately. Moreover, from definition (4.7) it follows that

$$\left(2\varphi_h^n - Z_h^n, \phi\right)_h = \left(\varphi_h^n, \phi\right)_h - \rho \left(\mu_h^n - \psi_2'(\varphi_h^{n-1}) - \mathcal{N}'(\varphi_h^{n-1}), \phi\right)_h + \rho\gamma^2 \left(\nabla\varphi_h^n, \nabla\phi\right)_{L^2(\Omega)} \tag{4.9}$$

We now adopt an iterative procedure, in the index k, using (4.7)-(4.9) and providing an analogue of the active nodes set $J_+(\varphi_h^{n-1})$ of the computational mesh, where $\varphi_h^{n-1} > 10^{-6}$ is meant for $\varphi_h^{n-1} > 0$. Starting from

$$\begin{aligned}\varphi_h^{n,0} &= \varphi_h^{n-1} \\ \mu_h^{n,0} &= \mu_h^{n-1},\end{aligned}$$

the algorithm consists of the following steps:

(1) Find $Z_h^{n,k} \in S_h$ using (4.7), such that $\forall\phi \in S_h^+$

$$\begin{aligned}\left(Z_h^{n,k}, \phi\right)_h = &\left(\varphi_h^{n,k}, \phi\right)_h + \rho \left(\mu_h^{n,k} - \psi_2'(\varphi_h^{n-1}) - \mathcal{N}'(\varphi_h^{n-1}), \phi\right)_h \\ &- \rho\gamma^2 \left(\nabla\varphi_h^{n,k}, \nabla\phi\right)_{L^2(\Omega)} .\end{aligned}$$

(2) As intermediate step, find $\varphi_h^{n,k+\frac{1}{2}} \in S_h^+$ such that

$$\varphi_h^{n,k+\frac{1}{2}}(\mathbf{x}_j) = \varphi_h^{n-1}(\mathbf{x}_j) \qquad j \in J_0(\varphi_h^{n-1}) \tag{4.10a}$$

$$\left(\varphi_h^{n,k+\frac{1}{2}} + \rho\psi_1'\left(\varphi_h^{n,k+\frac{1}{2}}\right) - Z_h^{n,k}, \phi - \varphi_h^{n,k+\frac{1}{2}}\right)_h \geq 0, \tag{4.10b}$$

where the inequality, which is actually (4.8), is valid $\forall \phi \in S_h^+$ and must be solved on the set of active nodes $J_+(\varphi_h^{n-1})$. This scalar inequality is thereby a projection problem on each active node and it can be solved through the *Projected Gradient Descent Method* (PGD), introducing a fixed point iteration of index l, another relaxation parameter $\omega > 0$ and starting from $\varphi_h^{n,k+\frac{1}{2},0} = \varphi_h^{n,k}$. The parameter ω is determined as follows

$$\begin{aligned}
&\varphi_h^{n,k+\frac{1}{2},l+1}(\mathbf{x}_j) = \\
&= P_{\mathbb{R}^+}\left[\varphi_h^{n,k+\frac{1}{2},l}(\mathbf{x}_j) - \omega\left(\varphi_h^{n,k+\frac{1}{2},l}(\mathbf{x}_j) + \rho\psi_1'\left(\varphi_h^{n,k+\frac{1}{2},l}(\mathbf{x}_j)\right) - Z_h^{n,k}\right)\right] \\
&= \max\left\{0, \varphi_h^{n,k+\frac{1}{2},l}(\mathbf{x}_j) - \omega\left(\varphi_h^{n,k+\frac{1}{2},l}(\mathbf{x}_j) + \rho\psi_1'\left(\varphi_h^{n,k+\frac{1}{2},l}(\mathbf{x}_j)\right) - Z_h^{n,k}\right)\right\}.
\end{aligned}$$

so that the iterations converge using the Polyak Method [49].
Observe that the application of the PGD Method is possible since the first operand in the lumped scalar product of (4.10b) is monotone, given the convexity of the functions involved. If the error

$$\left\|\varphi_h^{n,k+\frac{1}{2},l+1} - \varphi_h^{n,k+\frac{1}{2},l}\right\|_{\ell^2}$$

is below a certain tolerance, we stop the cycle and set

$$\varphi_h^{n,k+\frac{1}{2}} = \varphi_h^{n,k+\frac{1}{2},l+1}.$$

(3) Find $(\varphi_h^{n,k+1}, \mu_h^{n,k+1}) \in S_h^+ \times S_h$ by solving the following system:

$$\begin{cases}
\dfrac{1}{\triangle t}\left(\varphi_h^{n,k+1}, \xi\right)_h + \left(\nabla\mu_h^{n,k+1}, \nabla\xi\right)_{L^2(\Omega)} = \dfrac{1}{\triangle t}\left(\varphi_h^{n-1}, \xi\right)_h \\
+ \left([1 - b(\varphi_h^{n-1})]\nabla\mu_h^{n,k}, \nabla\xi\right)_{L^2(\Omega)} \\
\left(\varphi_h^{n,k+1}, \phi\right)_h + \rho\gamma^2\left(\nabla\varphi_h^{n,k+1}, \nabla\phi\right)_{L^2(\Omega)} - \rho\left(\mu_h^{n,k+1}, \phi\right)_h \\
= \left(2\varphi_h^{n,k+\frac{1}{2}} - Z_h^{n,k} - \rho\psi_2'(\varphi_h^{n-1}) - \rho\mathcal{N}'(\varphi_h^{n-1}), \phi\right)_h
\end{cases} \tag{4.11}$$

for all $(\xi, \phi) \in S_h \times S_h^+$. The splitting

$$b(\varphi_h^{n-1})\nabla\mu_h^{n,k+1} = [1 - (1 - b(\varphi_h^{n-1}))]\nabla\mu_h^{n,k+1}$$

is not strictly necessary but enhances the convergence of the numerical method.

(4) Finally, if the error

$$\left\| \varphi_h^{n,k+1} - \varphi_h^{n,k} \right\|_{L^\infty(\Omega)}$$

is below a given threshold, we set

$$\varphi_h^n = \varphi_h^{n,k+1}$$
$$\mu_h^n = \mu_h^{n,k+1},$$

otherwise the k-iteration must restart.

4.3. Numerical results

In the following, we discuss the numerical results of three test cases in a two-dimensional domain.

In the first test case, we study the effects of elasticity on the spinodal decomposition and coarsening dynamics adding a random perturbation on a uniform initial concentration of tumour cells in the metastable regime.

In the second test case, we will consider the merging of isolated circular tumour sub-domains immersed in a healthy tissue.

In the third test case, we consider the evolution of a circular tumor sub-domain, with initial concentration $\varphi_0 = 0.55$, immersed in a healthy tissue. For this case we assume that the tumour cells can proliferate following a logistic growth law, to illustrate the effects of the elastic nonlinear term on the tumour expansion.

In all the test cases, We will show the numerical results obtained by setting $k = 0$ and $k = 0.1$, and the dimensionless domain is $\Omega = (-3, 3) \times (-3, 3)$. The mesh is created choosing an uniform partition of 64 sub-intervals on each edge. The values of the parameters kept fixed during the simulations are reported in Table 1 and they originate from biological data settled in literature. We use the expression (2.11) for H_λ. To check the validity of the model, we make use of a *FreeFem++* code adapted from the one exploited in [1]. In particular, we added the handle functions to deal with the non-locality and, following the numerical algorithm presented in Section 4.2, we implemented an additional integral term in the definition of function $Z_h^{n,k}$. Moreover, an adaptive time step is implemented in order to avoid numerical errors due to an excessively long temporal pace. Since the support of the discrete solution can move at most of a length h at each time step, we want to guarantee that the solution in the passive nodes does not block the spreading of the non-zero discrete solutions in the active nodes, meaning that

$$\triangle t < \frac{h_{\min}}{v_{\max}},$$

where $h_{\min}$ is the smallest edge length among the elements of the mesh, and $v_{\max}$ is the maximum on Ω of the tumour expansion velocity, calculated from a Darcy-like law of the form

$$\mathbf{v} = -\frac{b(\varphi)}{\varphi} \nabla \mu$$

	Parameter description	Value
γ	Thickness of the diffuse interface	0.025 mm
ν	Tumour cells proliferation rate	2.5 day^{-1}
D	Friction coefficient	20 Pa · day · mm^{-2}
E	Young modulus of the cancerous phase	1 Pa
λ	Threshold for the presence of the elastic contribution	0.1
φ^*	Concentration value for mutual equilibrium of the cells	0.6
$\triangle t$	Temporal discretization parameter	0.000 625 day
ρ	Relaxation parameter for the first step	0.046875
ω	Relaxation parameter for the second step	0.0646
tol	Tolerance for the fixed point iterations	$5 \cdot 10^{-5}$

Table 1. Numerical model parameters and their values. The time step is chosen to be $\triangle t = 0.5\gamma^2$, while between the two relaxation parameters the following relation holds: $\omega = 0.2/(3 + 2\rho)$.

where $\varphi \neq 0$, and set to zero where $\varphi = 0$. In particular, we set

$$v_{\max} = \max_{\mathbf{x}_j} \left(|v_x(\mathbf{x}_j)| + |v_y(\mathbf{x}_j)| \right)$$

and we impose

$$\triangle t = \min \left(\frac{\gamma^2}{2}, \frac{h_{\min}}{2v_{\max}} \right).$$

For the last test case, we introduce a source term of the form

$$\nu \varphi_h^{n-1}(1 - \varphi_h^{n-1})$$

on the right hand side of equation (4.11) in order to illustrate the effects of the elastic nonlinear effects on the tumour expansion. The parameter ν represents the tumour cells proliferation rate.

4.3.1. Test Case 1: Coarsening dynamics. In Figure 2 we report the initial condition $\phi_0 = 0.05 \pm 0.025\delta$, where δ is a random perturbation uniformly distributed in the interval $[0, 1]$. We also report the value of the mass of the solution,

$$m := \frac{1}{|\Omega|}(\varphi_h^n, 1)_h.$$

In Figure 3 we show the plots of ϕ_h^n at different time points during the phase separation dynamics and the coarsening dynamics of the separated domain sub-regions. We compare side by side the case setting $k = 0$, with no elasticity of the tumor tissue, and the case setting $k = 0.1$, accounting for nonlocal elastic effects. In Figure 3, we remark that the mass of the solution is conserved both for the cases with $k = 0$ and $k = 0.1$. As expected

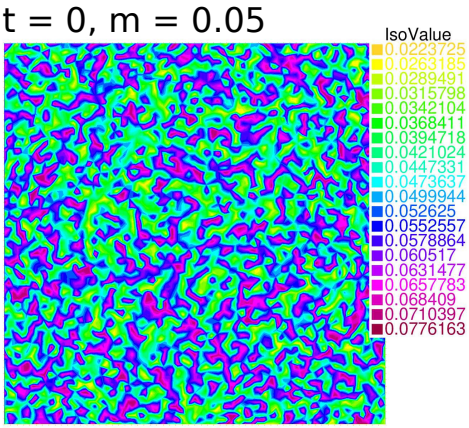

Figure 2. Initial condition $\phi_0 = 0.05 \pm 0.025\delta$ for Test Case 1.

(see e.g. [1]), the phase separation dynamics in the case $k = 0$ consists in the formation of circular clusters with $\varphi \sim \varphi^*$ immersed in a bath with $\phi \equiv 0$. In the case $k = 0.1$, we observe that the phase separation dynamics is slower and that the interface regions between separated phases are wider than in the case without elasticity. Also, the nonlocal elastic term increase the average length of the cluster domains and enforces a resistance against relaxation to the background value $\varphi \equiv 0$ during the whole phase separation.

4.3.2. Test Case 2: Merging dynamics. The initial condition is given by $\varphi_0 = 0.55(\chi_{B1} + \chi_{B2})$, where χ_{B1} and χ_{B2} are the characteristic functions of two circular regions placed symmetrically along the x direction. In Figure 4 we show the plots of φ_h^n at different time points throughout the merging dynamics, comparing the results obtained setting $k = 0$ and $k = 0.1$. We observe from Figure 4 that, the initial circular clusters for $k = 0$ evolve with interacting tips initially oriented along the bisecting directions of the plane, finally merging into the equilibrium shape of an ellipse with the major axis oriented along the x axis. This merging dynamics is consistent with a minimization of the tumour boundaries driven by nonlocal short-range intercellular potential only. In the case $k = 0.1$, the circular clusters interact only weakly to the further elastic confinement, not merging during the observed time interval considered. The numerical results for the case with tissue elasticity share a similar physical interpretation with the numerical results reported in [48] for interacting hard precipitates in a linear isotropic non-homogeneous elastic medium, where the elastic modulus associated to the phase $\varphi \equiv 1$ is higher than the elastic modulus associated to the phase $\varphi \equiv 0$. Indeed, the aforementioned numerical results in [48] show a repulsion between the precipitates, with lack of mutual interaction.

4.3.3. Test Case 3: Elastic effects on tumour expansion. The initial condition $\varphi_0 = 0.55$ is located on a circular shape of radius $r = 0.4$ centred in the square domain Ω. Outside of the circle, we initially set $\varphi_0 = 0$ uniformly. In Figure 5, we compare the numerical

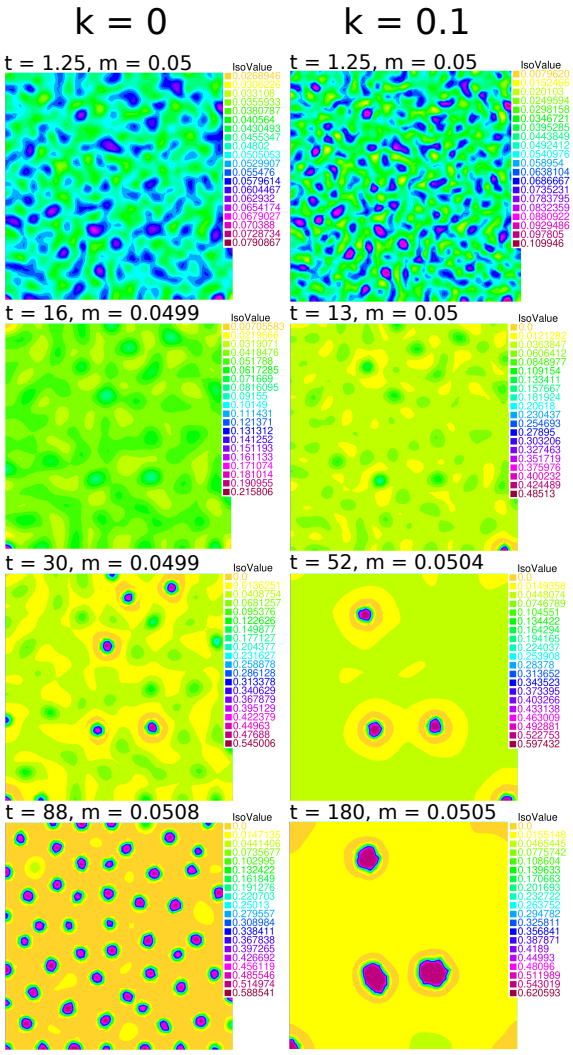

Figure 3. Plot of ϕ_h^n at different time points for Test Case 1, in the cases $k = 0$ (first column) and $k = 0.1$ (second column).

solutions at three different time instants to show the differences in the moving boundary and the fact that the tumour mass m continues to increase due to growth for the cases $k = 0$ and $k = 0.1$.

Setting $k = 0$, only the logistic proliferation rate, the cell-cell adhesion forces, and the intermixing boundary forces between the tumour and the healthy tissue, compete for driving the expansion of the tumour boundary. Setting $k = 0.1$, we find that the support of the solution is still expanding, but the added elastic contribution, causes a inhibition of the

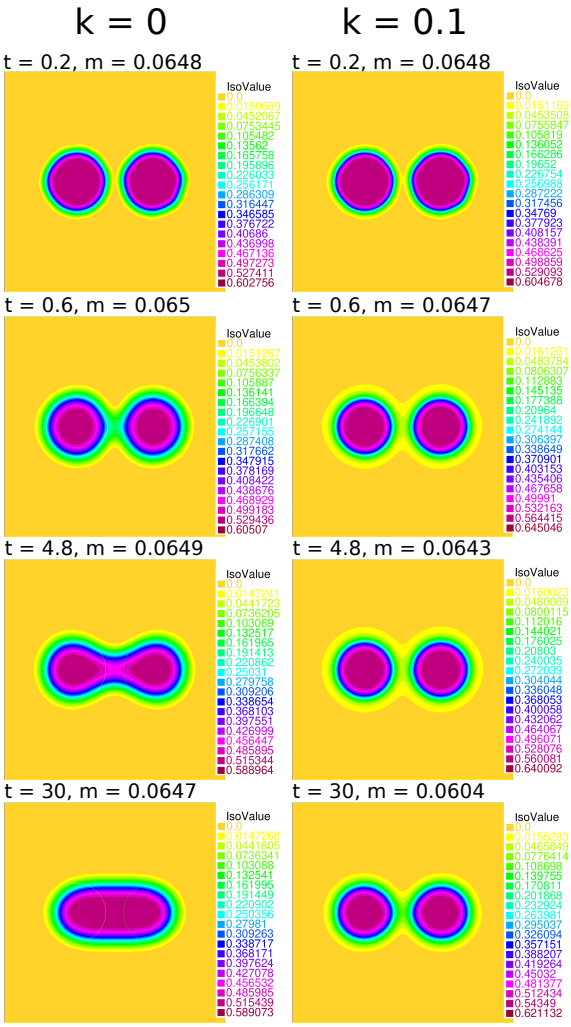

Figure 4. Plot of φ_h^n at different time points for Test Case 2, setting $k = 0$ (first column) and $k = 0.1$ (second column).

domain expansion where $\varphi > \varphi*$ (the core). This also results into an increase of the tumour volume fraction in the core. From the legends, we observe that the maximum concentration of cancerous cells is higher in the case $k = 0.1$ for any sampled time. For instance, in the last row of Figure 5, the maximum concentration with elasticity is $\varphi_{\max} = 0.784202$ against the value $\varphi_{\max} = 0.688042$ of the case without elasticity. Thus, as the nonlocal elastic contribution is added, the motion of the support is hindered. Finally, we plot in Figure 6 the evolution of the concentration over time with respect to the radial coordinate,

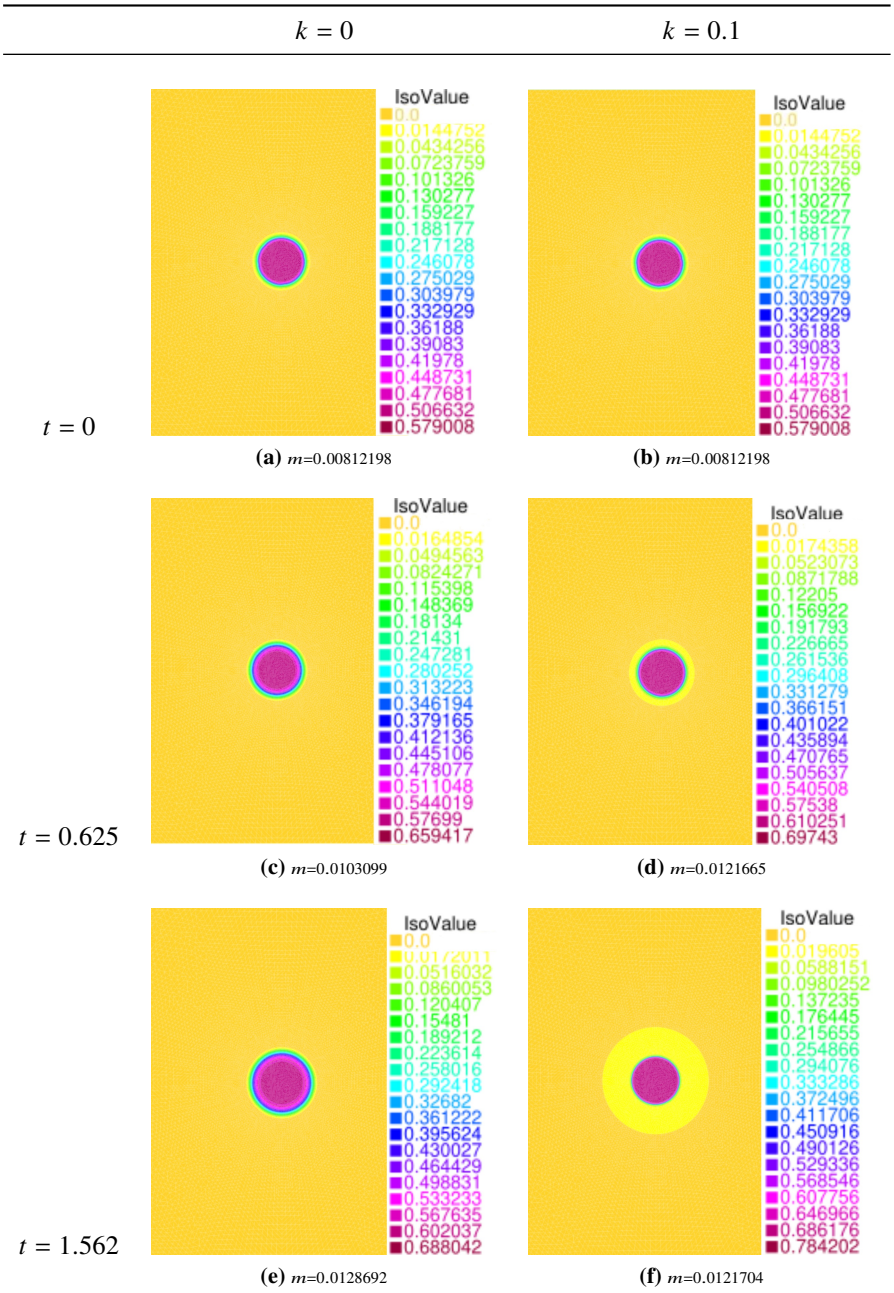

(a) m=0.00812198 **(b)** m=0.00812198

(c) m=0.0103099 **(d)** m=0.0121665

(e) m=0.0128692 **(f)** m=0.0121704

Figure 5. Test cases: comparison of the evolution of the tumor mass sampled at times $t = 0$, 0.625 and 1.250 for increasing values of $k = 0$ and $k = 10^{-1}$.

comparing once again the cases $k = 0$ and $k = 0.1$, but adding also the two intermediate values $k = 0.001$ and $k = 0.01$ for comparison. We take into consideration only the four more advanced time instants of the simulation, namely $t = 0.625$, $t = 0.937$, $t = 1.250$ and $t = 1.562$. It is worth noting that the trend of the concentration is smoother when $k = 0$, whilst the elastic contribution causes the concentration to increase sharply close to the boundary of the cancerous phase. Observing the tails of the plots in the second row of Figure 6, corresponding to $t = 1.250$ and $t = 1.562$, we confirm that increasing the elastic constant causes the concentration to be higher in the transition area between the cancerous phase and the healthy phase.

5. Conclusion and future works

In this work we have considered a Cahn–Hilliard equation with degenerate mobility and single-well potential, adding a membrane-like elastic effect due to tissue displacement caused by the expansion of the tumour boundary. This phenomenon has been modelled by introducing a nonlocal term, extended to the whole domain Ω, in the expression of the Landau grand potential. We used a standard mixture theory approach to derive a complete model consisting of a continuity equation whose flux, multiplied by a mobility term, is the gradient of a chemical potential accounting for the different kinds of energies involved. In particular, we introduced a diffuse interface, instead of treating the boundary as a sharp surface, so as to avoid the interface tracking in the numerical analysis. Completing the model with initial and boundary conditions, we then proceeded to establish the existence of weak solutions to the corresponding initial and boundary value problem. Starting from the existence and H^3-regularity of a weak solution of a regularized problem, to handle the sets of mobility degeneracy and potential singularity, we then proved two *a priori* estimates uniform with respect to the regularization parameters. The entropy estimate guaranteed the preservation of the positivity of the initial datum, while the energy estimate ensured that the saturation level for the cells concentration is reached. Thanks to both the estimates, we have been able to pass to the limit, for regularization parameters going to zero, in the regularized problem and obtain the existence of a weak solution to the original problem. This step has been quite delicate: in the bi- and three-dimensional cases, we could not prove the Hölder continuity of the regularized solution and thus the uniform convergence of the regularized solution to a solution of the original problem could not be guaranteed. For this reason, we introduced a different type of weak solution and proved the boundedness of the entire flux function (see [30] for more details on this strategy).

As for the numerical part, we had to overcome some difficulties in the discretization of the problem. First of all, the positivity property that the continuous solution inherits from the initial datum, guaranteed by the entropy estimate, is not preserved at the discrete level, forcing the introduction of a variational inequality to impose the positivity as a constraint. Furthermore, the non-uniqueness of the continuous solution may lead to nonphysical discrete solution with fixed support: to circumvent this problem, we introduced the discrete

Concentration along the radial coordinate in four different time instants

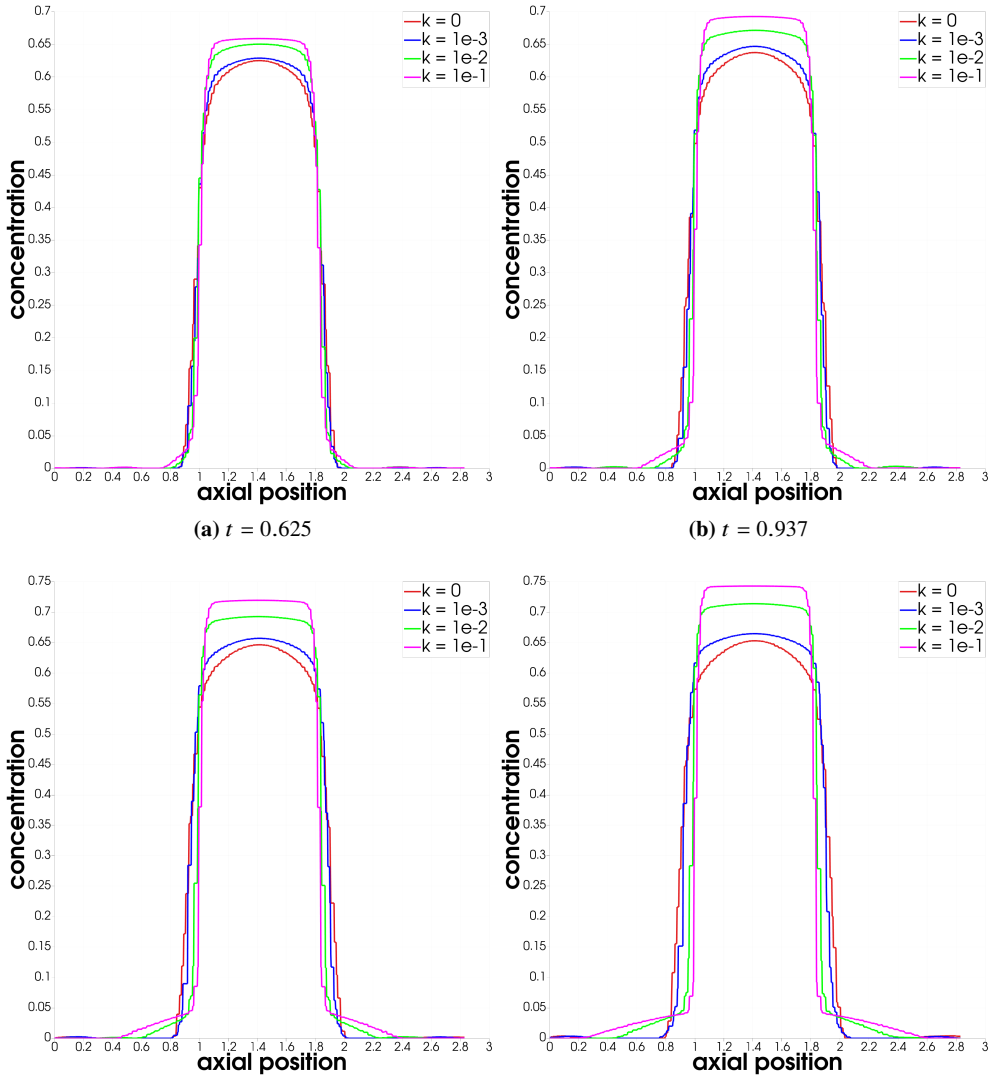

(a) $t = 0.625$ **(b)** $t = 0.937$

(c) $t = 1.250$ **(d)** $t = 1.562$

Figure 6. The value of the concentration is plotted with respect to the radial coordinate, comparing the cases $k = 0$, $k = 10^{-3}$, $k = 10^{-2}$ and $k = 10^{-1}$ in four different time steps: $t = 0.625$, $t = 0.937$, $t = 1.250$ and $t = 0.1562$.

inner product and performed a partition of the nodes of the mesh into passive and active nodes. We described a numerical algorithm to solve the variational inequality at each time step, explicitly treating the non-locality. Finally, we have performed various numerical simulations on a simplified square geometry to test the validity of the algorithm, setting physically meaningful values for the model parameters from the literature. In particular, we showed the effects of elasticity on the spinodal decomposition, on the merging of isolated subdomains of cancerous phase, and on the evolution of a circular region of tumour under the effect of a logistic proliferation rate of the cancer cells. The results are promising, but they suffer some limitations. First of all, the explicit treatment of the nonlocal elastic term forces the time step of the numerical scheme to be very small, resulting in long and heavy computations: the convergence of the fixed-point iterations is in this case very difficult to achieve. Moreover, to get more accurate information about the influence of the elasticity on the moving support of the cancerous phase, the concentration in the transition area and the maximum concentration on the core of the tumour, we should examine the behaviour on a longer time scale. For future developments, an implicit treatment of the nonlocal term could be proposed to reduce the numerical complexity, relaxing also the requirements on the time step. Moreover, since it is always possible to decompose a function into its convex and concave parts, future studies will investigate the optimality of such a splitting. From the modelling viewpoint, more refined elastic models may be sought to describe other boundary elastic effects, for instance depending on the mean or Gaussian curvature of the boundary of the cancerous phase, and/or introducing a penalization on the first (or the second) fundamental form of the surface of the tumour. Finally, a further development will concern the coupling of the nonlocal Cahn–Hilliard equation studied in this work with other biologically relevant features of tumour growth, such as the diffusion/uptake of a nutrient and/or the response to anti-cancer therapies.

Acknowledgements. M. Grasselli and A. Agosti are members of Gruppo Nazionale per l'Analisi Matematica, la Probabilità e le loro Applicazioni (GNAMPA), Istituto Nazionale di Alta Matematica (INdAM). P. Ciarletta is member of Gruppo Nazionale per la Fisica Matematica (GNFM), INdAM.

Funding. R. Bardin acknowledges the support by NWO via Grant OCENW.KLEIN.183; A. Agosti, P. Ciarletta and M. Grasselli acknowledge the support of MIUR through the PRIN Grant 2020F3NCPX "Mathematics for Industry 4.0 (Math4I4)". P. Ciarletta and M. Grasselli acknowledge the support by MUR, grant Dipartimento di Eccellenza 2023-2027.

References

[1] A. Agosti, P. F. Antonietti, P. Ciarletta, M. Grasselli, and M. Verani, A Cahn-Hilliard type equation with application to tumor growth dynamics. Math. Methods Appl. Sci. **40** (2017), 7598–7626

[2] A. Agosti, P. Colli, H. Garcke, and E. Rocca, A Cahn–Hilliard model coupled to viscoelasticity with large deformations. To appear in Commun. Math. Sci. (2022)
[3] S. M. Allen and J. W. Cahn, Ground state structures in ordered binary alloys with second neighbor interactions. Acta Metall. **20** (1972), 423–433
[4] D. Ambrosi and L. Preziosi, On the closure of mass balance models for tumour growth. Math. Models Methods Appl. Sci. **12** (2002), 737–754
[5] D. Anders and K. Weinberg, Numerical simulation of diffusion induced phase separation and coarsening in binary alloys. Comput. Mater. Sci. **50** (2011), 1359–1364
[6] J. W. Barrett and J. F. Blowey, Finite element approximation of a model for phase separation of a multi-component alloy with non-smooth free energy. Numer. Math. **77** (1997), 1–34
[7] J. W. Barrett, J. F. Blowey, and H. Garcke, Finite element approximation of the Cahn-Hilliard equation with degenerate mobility. SIAM J. Numer. Anal. **37** (1999), 286–318
[8] F. Bernis and A. Friedman, Higher order nonlinear degenerate parabolic equations. J. Differential Equations **83** (1990), 179–206
[9] A. Bertozzi, S. Esedoglu, and A. Gillette, Analysis of a two-scale Cahn–Hilliard model for binary image inpainting. Multiscale Model. Simul. **6** (2007), 913–936
[10] A. Bertozzi, S. Esedoglu, and A. Gillette, Inpainting of binary images using the Cahn-Hilliard equation. IEEE Trans. Image Process. **16** (2007), 285–291
[11] F. Boyer, A theoretical and numerical model for the study of incompressible mixture flows. Comput. & Fluids **31** (2002), 41–68
[12] C. Brangwynne, P. Tompa, and R. Pappu, Polymer physics of intracellular phase transitions. Nat. Phys. **11** (2015), 899–904
[13] H. Byrne and L. Preziosi, Modelling solid tumour growth using the theory of mixtures. Mathematical medicine and biology: a journal of the IMA **20** (2003), no. 4, 341–366
[14] H. Byrne and L. Preziosi, Modelling solid tumour growth using the theory of mixtures. Math. Med. Biol. **20** (2004), 341–366
[15] J. W. Cahn, On spinodal decomposition. Acta Metall. **9** (1961), 795–801
[16] J. W. Cahn, C. M. Elliott, and A. Novick-Cohen, The Cahn-Hilliard equation with a concentration dependent mobility: motion by minus the laplacian of the mean curvature. Eur. J. Appl. Math. **7** (1996), 287–301
[17] J. W. Cahn and J. E. Hilliard, Free energy of nonuniform system I. Interfacial free energy. J. Chem. Phys. **28** (1958), 258–267
[18] C. Chatelain, T. Balois, P. Ciarletta, and M. B. Amar, Emergence of microstructural patterns in skin cancer: a phase separation analysis in a binary mixture. New J. Phys. **13** (2011), 115013–115033
[19] C. Chatelain, P. Ciarletta, and M. B. Amar, Morphological changes in early melanoma development: influence of nutrients, growth inhibitors and cell-adhesion mechanism. J. Theor. Biol. **290** (2011), 46–59
[20] Y. Chen and J. Lowengrub, Tumor growth in complex, evolving microenvironmental geometries: a diffuse domain approach. J. Theor. Biol. **361** (2014), 14–30
[21] Y. Chen, S. Wise, and J. Shenoy, V.B. Lowengrub, A stable scheme for a nonlinear, multiphase tumor growth model with an elastic membrane. Int. J. Numer. Method. Biomed. Eng. **30** (2014), 726–754
[22] L. Cherfils, A. Miranville, and S. Zelik, The Cahn-Hilliard equation with logarithmic potentials. Milan J. Math. **79** (2011), 561–596

[23] M. Colombo, C. Giverso, E. Faggiano, C. Boffano, F. Acerbi, and P. Ciarletta, Towards the personalized treatment of glioblastoma: integrating patient-specific clinical data in a continuous mechanical model. PLoS One **10** (2015), no. 11, e0143032

[24] M. I. M. Copetti and C. M. Elliott, Numerical analysis of the Cahn-Hilliard equation with a logarithmic free energy. Numer. Math. **63** (1992), 39–65

[25] V. Cristini and J. Lowengrub, Multiscale modeling of cancer: an integrated experimental and mathematical modeling approach. Cambridge University Press, 2010

[26] A. Denis, C. Hesch, and K. Weinberg, Computational modeling of phase separation and coarsening in solder alloys. Int J Solids Struct **49** (2012), 1557–1572

[27] M. Doi, Onsager's variational principle in soft matter. J. Condens. Matter Phys. **23** (2011)

[28] E. Dolgin, What lava lamps and vinaigrette can teach us about cell biology. Nat. **555** (2018), 300–302

[29] R. Y. Dong and S. Granick, Reincarnations of the phase separation problem. Nat. Commun. **12** (2021), 911

[30] C. M. Elliott and H. Garcke, On the Cahn-Hilliard equation with degenerate mobility. SIAM J. Math. Anal. **27** (1994), 404–423

[31] C. M. Elliott and S. Zheng, On the Cahn–Hilliard equation. Arch. Ration. Mech. Anal. **96** (1996), 339–357

[32] J. Erlebacher, M. J. Aziz, A. Karma, N. Dimitrov, and K. Sieradzki, Evolution of nanoporosity in dealloying. Nat. **410** (2001), 450–453

[33] H. Ganapathy, E. Al-Hajri, and M. Ohadi, Phase field modeling of taylor flow in mini/macrochannels, part ii: Hydrodynamics of taylor flow. Chem. Eng. Sci. **94** (2013), 156–165

[34] H. Garcke, B. Kovács, and D. Trautwein, Viscoelastic Cahn-Hilliard models for tumour growth. Math. Models Methods Appl. Sci. **32** (2022), 2673–2758

[35] H. Garcke, K. F. Lam, and A. Signori, On a phase field model of Cahn–Hilliard type for tumour growth with mechanical effects. Nonlinear Anal. Real World Appl. **57** (2021), 103192

[36] G. Grün, Degenerate parabolic differential equations of fourth order and a plasticity model with non-local hardening. Z. Anal. Anwend. **14** (1995), 541–574

[37] G. Grün and M. Rumpf, Nonnegativity preserving convergent schemes for the thin film equation. Numer. Math. **87** (2000), 113–152

[38] M. Gurtin, Generalized Ginzburg-Landau and Cahn-Hilliard equations based on a microforce balance. Phys. D **92** (1996), 178–192

[39] M. Gurtin, D. Polignone, and J. Viñals, Two-phase binary fluids and immiscible fluids described by an order parameter. Math. Models Methods Appl. Sci. **6** (1996), 815–831

[40] M. Holmes, Mixture theories for the mechanics of biological tissues. RPI Web Book, 1995

[41] A. A. Hyman and K. Simon, Beyond oil and water-phase transitions in cells. Science **337** (2012), 1047–1049

[42] N. Kenmochi, M. Niezgódka, and I. Pawłow, Subdifferential operator approach to the Cahn-Hilliard equation with constraint. J. Differential Equations **117** (1995), 320–356

[43] E. Khain and L. Sander, Generalized Cahn-Hilliard equation for biological applications. Phys. Rev. E Stat. Nonlin. Soft Matter Phys. **77** (2005), 51–129

[44] V. V. Khatavkar, P. D. Anderson, and H. E. H. Meijer, On scaling of diffuse-interface models. Chem. Eng. Sci. **61** (2006), 2364–2378

[45] J. Kim, A continuous surface tension force formulation for diffuse-interface models. J. Comput. Phys. **204** (2005), 784–804

[46] J. Kim, Phase-field models for multi-component fluid flows. Commun. Comput. Phys. **12** (2012), 613–661

[47] J. Lennard-Jones, On the determination of molecular fields. -ii. from the equation of state of a gas. Proc. Math. Phys. Eng. Sci. **106** (1924), 463–477

[48] P. H. Leo, J. S. Lowengrub, and H. J. Jou, A diffuse interface model for microstructural evolution in elastically stressed solids. Acta Mater. **46** (1998), no. 6, 2113–2130

[49] E. S. Levitin and B. T. Polyak, Constrained minimization methods. USSR Comput. Math. and Math. Phys. **6** (1966), 1–50

[50] P. L. Lions and B. Mercier, Splitting algorithms for the sum of two nonlinear operators. SIAM J. Numer. Anal. **16** (1979), 964–979

[51] Q.-X. Liu, A. Doelman, V. Rottschafer, and M. de Jager, Phase separation explains a new class of self-organized spatial patterns in ecological systems. Proc. Natl. Acad. Sci. USA **110** (2013)

[52] J. Lowengrub and L. Truskinovsky, Quasi-incompressible Cahn-Hilliard fluids and topological transitions. Proc. Math. Phys. Eng. Sci. **454** (1998), 2617–2654

[53] J. S. Lowengrub, H. B. Frieboes, F. Jin, Y.-L. Chuang, X. Li, P. Macklin, S. M. Wise, and V. Cristini, Nonlinear modelling of cancer: bridging the gap between cells and tumours. Nonlinearity **23** (2009), no. 1, R1

[54] P. Lu, V. M. Weaver, and Z. Werb, The extracellular matrix: a dynamic niche in cancer progression. J. Cell. Biol. **196** (2012), no. 4, 395–406

[55] L. McMaster, Aspects of liquid-liquid phase transition phenomena in multicomponent polymeric systems. Adv. Chem. **142** (1975), 43–65

[56] A. Miranville, The Cahn-Hilliard equation: Recent advances and applications. CBMS-NSF regional conference series in applied mathematics, Society for Industrial and Applied mathematics (SIAM), 2019

[57] D. Molin and R. Mauri, Spinodal decomposition of binary mixtures with composition-dependent heat conductivities. Chem. Eng. Sci. **63** (2008), 2402–2407

[58] J. Park, R. Mauri, and P. Anderson, Phase separation of viscous ternary liquid mixtures. Chem. Eng. Sci. **80** (2012), 270–278

[59] B. Perthame and A. Poulain, Relaxation of the Cahn-Hilliard equation with singular single-well potential and degenerate mobility. Eur. J. Appl. Math. **32** (2020), 89–112

[60] L. Preziosi, Cancer modelling and simulation. CRC Press, 2003

[61] G. Schimperna and S. Zelik, Existence of solutions and separation from singularities for a class of fourth order degenerate parabolic equations. Trans. Amer. Math. Soc. **365** (2013), 3799–3829

[62] S. Schulz, Phase-field simulations of multi-component solidification and coarsening based on thermodynamic datasets. KIT Scientific Publishing, 2017

[63] J. Simon, Compact sets in the space $L^p(0,T;B)$. Ann. Mat. Pura Appl. (4) **146** (1987), 65–96

[64] S. Tremaine, On the origin of irregular structure in Saturn's rings. Astron. J. **125** (2002), 894–901

[65] P. A. Wijeratne, J. H. Hipwell, D. J. Hawkes, T. Stylianopoulos, and V. Vavourakis, Multiscale biphasic modelling of peritumoural collagen microstructure: The effect of tumour growth on permeability and fluid flow. PloS One **12** (2017), no. 9, e0184511

[66] Y. Zeng and M. Z. Bazant, Phase separation dynamics in isotropic ion-interaction particles. SIAM J. Appl. Math. **74** (2014), 980–1004

[67] C. Zhou and S. Kumar, Two-dimensional two-layer channel flow near a step. Chem. Eng. Sci. **81** (2012), 38–45

Abramo Agosti
Dipartimento di Matematica 'F. Casorati', Università degli Studi di Pavia, Via Ferrata 5, 27100 Pavia, Italy; abramo.agosti@unipv.it

Riccardo Bardin
Department of Applied Mathematics, MACS Group, University of Twente, P.O. Box 217, 7500 AE Enschede, The Netherlands; r.bardin@utwente.nl

Pasquale Ciarletta
MOX Laboratory, Dipartimento di Matematica, Politecnico di Milano, Via E. Bonardi 9, 20133 Milano, Italy; pasquale.ciarletta@polimi.it

Maurizio Grasselli
Dipartimento di Matematica, Politecnico di Milano, Via E. Bonardi 9, 20133 Milano, Italy; maurizio.grasselli@polimi.it

MOX Technical Reports, last issues

Dipartimento di Matematica
Politecnico di Milano, Via Bonardi 9 - 20133 Milano (Italy)

78/2023 Antonietti, P.F.; Bonizzoni, F.; Corti, M.; Dall'Olio, A.
Discontinuous Galerkin for the heterodimer model of prion dynamics in Parkinson's disease

77/2023 Fumagalli, I.; Corti, M.; Parolini, N.; Antonietti, P. F.
Polytopal discontinuous Galerkin discretization of brain multiphysics flow dynamics

76/2023 Ieva, F.; Galliani, G.; Secchi, P.
The impact of public transport on the diffusion of COVID-19 pandemie in Lombardy during 2020

74/2023 Pidò, S.; Pinoli, P.; Crovari, P.; Ieva, F.; Garzotto, F.; Ceri, S.
Ask Your Data—Supporting Data Science Processes by Combining AutoML and Conversational Interfaces

75/2023 Archetti, A.; Ieva, F.; Matteucci, M.
Scaling survival analysis in healthcare with federated survival forests: A comparative study on heart failure and breast cancer genomics

71/2023 Conni, G.; Piccardo, S.; Perotto, S.; Porta, G.M.; Icardi, M.
HiPhome: HIgh order Projection-based HOMogEnisation for advection diffusion reaction problems

70/2023 Ragni, A.; Ippolito, D.; Masci, C.
Assessing the Impact of Hybrid Teaching on Students' Academic Performance via Multilevel Propensity Score-based techniques

69/2023 Ferro, N.; Micheletti, S.; Parolini, N.; Perotto, S.; Verani, M.; Antonietti, P. F.
Level set-fitted polytopal meshes with application to structural topology optimization

68/2023 Vitullo, P.; Colombo, A.; Franco, N.R.; Manzoni, A.; Zunino, P.
Nonlinear model order reduction for problems with microstructure using mesh informed neural networks

67/2023 Conti, P.; Guo, M.; Manzoni, A.; Hesthaven, J.S.
Multi-fidelity surrogate modeling using long short-term memory networks